THE CHARACTERIZATION OF THE KINETICS OF *CHLAMYDIA MURIDARUM* INFECTION IN DEFINED REGIONS OF THE MURINE GENITAL TRACT

APPROVED BY SUPERVISING COMMITTEE:

_____
Bernard Arulanandam, Ph.D., Chair

_____
Neal Guentzel, Ph.D.

_____
Hans Heidner, Ph.D.

Accepted: _____
Dean, Graduate School

DEDICATION

This thesis is dedicated to Brian Heft, the man whose love, support, and inspiration were pivotal in the completion of this manuscript. It is also dedicated to my mom, who has never failed to provide love and encouragement in the support of my endeavors.

THE CHARACTERIZATION OF THE KINETICS OF *CHLAMYDIA MURIDARUM* INFECTION IN DEFINED REGIONS OF THE MURINE GENITAL TRACT

by

ILEA ESKILDSEN, B.S.

THESIS
Presented to the Graduate Faculty of
The University of Texas at San Antonio
In partial Fulfillment
Of the Requirements
For the Degree of

MASTER OF SCIENCE IN BIOLOGY

THE UNIVERSITY OF TEXAS AT SAN ANTONIO
College of Sciences
Department of Biology
August 2008

Report Documentation Page

Form Approved
OMB No. 0704-0188

1. REPORT DATE	2. REPORT TYPE	3. DATES COVERED
01 AUG 2008	**N/A**	**-**

4. TITLE AND SUBTITLE	5a. CONTRACT NUMBER
The Characterization Of The Kinetics Of Chlamydia Muridarum Infection In Defined Regions Of The Murine Genital Tract	5b. GRANT NUMBER
	5c. PROGRAM ELEMENT NUMBER
6. AUTHOR(S)	5d. PROJECT NUMBER
	5e. TASK NUMBER
	5f. WORK UNIT NUMBER
7. PERFORMING ORGANIZATION NAME(S) AND ADDRESS(ES) **The University of Texas at San Antonio College of Sciences Department of Biology**	8. PERFORMING ORGANIZATION REPORT NUMBER
9. SPONSORING/MONITORING AGENCY NAME(S) AND ADDRESS(ES) **AFIT/ENEL Wright-Patterson AFB, OH**	10. SPONSOR/MONITOR'S ACRONYM(S)
	11. SPONSOR/MONITOR'S REPORT NUMBER(S) **Cl09-0026**

12. DISTRIBUTION/AVAILABILITY STATEMENT
Approved for public release, distribution unlimited

13. SUPPLEMENTARY NOTES

14. ABSTRACT

15. SUBJECT TERMS

16. SECURITY CLASSIFICATION OF:			17. LIMITATION OF ABSTRACT	18. NUMBER OF PAGES	19a. NAME OF RESPONSIBLE PERSON
a. REPORT	b. ABSTRACT	c. THIS PAGE			
unclassified	**unclassified**	**unclassified**	**UU**	**62**	

ACKNOWLEDGEMENTS

I thank Dr. Bernard Arulanandam, Dr. Neal Guentzel, and Dr. Hans Heidner for serving as members of my committee and for providing invaluable support, guidance, and expertise. I thank Dr. Ashlesh Murthy, Heather Ray, Marcus King, and the entire Arul Lab for their expertise and support in completing this research. Additionally, I thank the Air Force Institute of Technology for providing funding of tuition for my course of study, and for the United States Air Force Academy Department of Biology for nominating me to receive the scholarship that afforded me this opportunity.

The views expressed in this article are those of the author and do not reflect the official policy or position of the United States Air Force, Department of Defense, or the U.S. Government.

August 2008

THE CHARACTERIZATION OF THE KINETICS OF *CHLAMYDIA MURIDARUM* INFECTION IN DEFINED REGIONS OF THE MURINE GENITAL TRACT

Ilea Eskildsen, M.S.
The University of Texas at San Antonio, 2008

Supervising Professor: Bernard Arulanandam, Ph.D.

Infection with *Chlamydia trachomatis* is the most common bacterial sexually transmitted disease worldwide, and leads to pathological sequelae including pelvic inflammatory disease and infertility. The continued increase in incidence rates of genital chlamydial infection over the last decade underscores a need for comprehensive understanding of the infection kinetics, host immune response, and disease pathogenesis. A mouse model of genital *Chlamydia muridarum* infection is generally employed in such studies, with most studies relying upon the enumeration of bacterial numbers from vaginal swab material to assess the kinetics of infection. Given the differences in tissue anatomy, hormonal regulation, and immune response among different genital regions, it is possible that kinetics of chlamydial infection as determined by vaginal swabbing may not accurately reflect the kinetics in other regions of the genital tract. In this study, we directly evaluated the kinetics of bacterial ascent into, and clearance from, defined regions of the reproductive tract using highly sensitive quantitative real-time PCR for the detection of *Chlamydia* genomes. The results of our study show that kinetics of chlamydial infection in different regions of the genital tract are comparable, with high numbers of organisms from day 3 through 18, and subsequent progressive reduction leading to complete clearance of infection around 30 days after challenge. The results also exhibit differences in the numbers of chlamydial organisms between different defined regions. Collectively, the results of this study

provide in-depth insight into the kinetics of genital *Chlamydia muridarum* infection in defined regions of the murine female reproductive tract.

TABLE OF CONTENTS

LIST OF FIGURES

LIST OF FIGURES (continued)

INRODUCTION

Chlamydia trachomatis is the most common bacterial sexually transmitted disease worldwide. With an estimated 90 million new infections worldwide each year (1) and over one million new cases in the U.S. in 2006 alone (2), infection with *C. trachomatis* is a serious public health concern. While effective antimicrobial treatment is available, a majority of infections remain asymptomatic (70-90% of women and 30-50% of men) (3) and are not treated. Untreated infections can lead to serious sequelae such as pelvic inflammatory disease, ectopic pregnancy and infertility (3). Additionally, the prevalence of genital chlamydial infections has continually increased over the last decade despite enhanced screening and public health programs (3). The rising prevalence of the disease and the serious sequelae underscore the need for a greater understanding of the disease process in order to design efficacious intervention strategies.

The murine model of genital chlamydial infection is widely used for study of the pathogenesis and immunity against this organism (4). Most studies of *Chlamydia* infection in mice assess the bacterial burden based on the collection of swab material from the vagina (5-8). However, the initial infection occurs in the lower genital tract, followed by ascent of organisms into the upper reproductive tract (3, 4, 9). The female reproductive tract presents a complex environment with the lower reproductive tract colonized by normal flora and exposed to the environment, while the upper reproductive tract (above the cervix) is essentially sterile (3). Furthermore, the immunology of the reproductive tract is precisely regulated by the ovarian hormones oestradiol and progesterone and varies throughout the menstrual cycle (10). Given the differences in the anatomy of the different regions of the reproductive tract and how they may influence chlamydial infection, the determination of vaginal chlamydial shedding alone may not

provide comprehensive information about the kinetics of chlamydial infection in the entire reproductive tract.

In this study, we directly evaluated the kinetics of bacterial ascent and clearance in the various defined regions of the reproductive tract of mice at multiple time-periods following intravaginal (i.vag.) chlamydial challenge using highly sensitive quantitative real-time PCR. The results of our study demonstrate that quantitative real-time PCR is a reliable and sensitive method for detecting the presence of chlamydial organisms, and that the kinetics of chlamydial infection in the vagina are comparable to that in the upper genital tract. Additionally, we found evidence on the differential distribution in the numbers of chlamydial organisms in different defined regions of the reproductive tract.

Chlamydia - Background and Overview

Chlamydia are a group of Gram negative obligate intracellular bacteria. There are four commonly recognized species of *Chlamydia: C. trachomatis, C. psittaci, C. pneumonia, and C. pecorum* (4). The mouse pneumonitis strain of *C. trachomatis* (formerly designated MoPn), was recently designated as a separate species and is known as *C.muridarum*. *C. psittaci* and *C. pecorum* are pathogens of birds and lower animals, with humans being only ancillary hosts, whereas *C. pneumoniae* and *C. trachomatis* are primarily human pathogens (4). *C. pneumoniae* causes acute respiratory infections and has been associated with cardiovascular disease (4). *C. trachomatis* is a strict pathogen of oculogenital epithelial cells. Ocular infection with *C. trachomatis* causes trachoma (the leading cause of preventable blindness), while genital infection is the leading cause of bacterial sexually transmitted diseases worldwide. There are 15 different serovars of *C. trachomatis.* Serovars A, B, Ba, and C cause trachoma, and serovars D to K and L1 to L3 cause sexually transmitted infections. Serovars L1, L2, and L3 cause lymphogranuloma venereum (LGV), whereas serovars D to K cause cervicitis, urethritis, and the associated complications of more severe diseases such as endometritis, salpingitis and pelvic inflammatory disease (PID) in women (4). This study is focused on the sexually transmitted disease caused by *Chlamydia trachomatis* in the female reproductive tract. *C. muridarum* is closely related to *C. trachomatis* and produces a genital infection in mice that is similar to human infection with *C. trachomatis* (4). It has therefore been used extensively for *in vivo* studies and is the species used in this study.

Chlamydia trachomatis – Developmental Cycle

Chlamydiae possess a unique biphasic developmental cycle (4). The extracellular form is an elementary body (EB), and the intracellular form is termed a reticulate body (RB). EBs are infectious, but metabolically inactive, whereas RBs are metabolically active, but non infectious. While the exact method of entry has yet to be fully understood, it is known that *Chlamydia* is endocytosed into clathrin coated pits (4, 11). There also is evidence to show that the initial interactions of EBs with host cells may occur via reversible, electrostatic interactions with heparin sulfate-like glycosaminoglycans (12). Upon entry into the host cell, *Chlamydia* secrete proteins and cause signaling events which play a role in inhibiting the fusion of the lysosome with the phagosome (4), allowing the EB to escape the death that would normally occur by this host defense mechanism. The architecture of the endosome is then remodeled into an inclusion. Inside the inclusion, EBs undergo changes to become RBs. The RBs divide by binary fission and reorganize into EBs approximately for about 18-24 hours after attachment. After 24-30 hr, phagolysosomal fusion occurs, and infectious EBs are released accompanied by death of the host cell (13). Upon release from the cell, EBs may infect other cells and continue the cycle (13).

Murine Model of Infection – *Chlamydia muridarum*

Due to the limitations of studying *C. trachomatis* infection in humans, various animals models have been used to understand the pathogenesis and immunity to genital chlamydial infection (14). Specifically, infection has been characterized in various primates (rhesus and grivet monkey, pig-tailed macaques, and marmosets), as well as in mice (14). While infection in primates most closely mimics that in humans, the use of this model for extensive studies is constrained by financial considerations (14).

Murine infection with *C. muridarum* is currently the most widely used model to study *Chlamydia* infections *in vivo*. *C. muridarum* is used in place of *C. trachomatis* because murine infection with *C. muridarum* produces a course of infection and pathology that closely mimics human infection with *C. trachomatis*, whereas murine infection with *C. trachomatis* does not.

Host tropism and differences in course of infection are attributed to the fact that *C. trachomatis* and *C. muridarum* have different means of evading the host IFN-γ mediated immune response (15). In humans, IFN-γ stimulates the production of indoleamine-3-dioxygenase (IDO) which has the effect of depleting tryptophan and starving *Chlamydia* (15). *C. trachomatis* is able to evade this host response because it contains a functional tryptophan synthase, allowing it to produce its own food source and establish a productive infection in the human host. *C. muridarum* lacks a functional tryptophan synthase and consequently is unable to cause infection in humans (15). In mice, the IFN-γ response is independent of IDO, and *C. trachomatis* is susceptible to the effects of the immune response, while *C. muridarum* is able to avoid the murine IFN-γ response, resulting in its ability to establish a productive infection in mice (15).

Murine infection with *C. trachomatis* results in an infection of short duration characterized by low infectious load, minimal submucosal inflammation and no significant post-infection sequelae – making it a poor model for studying *Chlamydia* infections. On the other hand, intravaginal inoculation with *C. muridarum* produces an infection that ascends the reproductive tract, with mice generally resolving the infection in about 4 weeks (4). Following resolution of the primary infection, most mice develop long-lasting protective immunity with secondary infections being of much shorter duration (4). Hydrosalpinx, defined as oviduct dilatation and luminal filling with a clear serous fluid (16), accompanied by infertility is a common post-infection sequelae, and similar pathology is observed in humans (4).

Some differences between murine infection with *C. muridarum* and human infection with *C.* trachomatis are the length of infection, and the development of protective immunity. Infections in humans can last for months before spontaneous clearance (mice resolve the infection in about 4 weeks) (4). As stated early, mice develop protective immunity to *C. muridarum* following primary challenge, whereas humans are susceptible to multiple rounds of infection with *C. trachomatis* (17). Although there are noted differences (above), the immune response produced after *C. muridarum* challenge strongly resembles that seen in human infection with *C. trachomatis,* and with the similarity in the development of pathology, is the main reason for the use of the murine model of infection. Collectively, murine infection with *C. muridarum* is not a perfect model, but presents a suitable method for use in developing our understanding of the immune response and pathogenesis of *C. trachomatis* infection.

Immunobiology

The immunobiology of *Chlamydia* infection is complex in that the host immune response is both protective and pathological (7). Various studies have established the components of the immune system that are essential for resolution of infection, but a definitive answer to the cause of pathology remains to be found.

Upon primary genital chlamydial infection, MHC class II dependent Th1 immune responses, including IFN-γ production and antigen-specific $CD4^+$ T cells, have been reported to play an important role in the establishment of protective immunity (4, 18). Additionally, adoptive transfer of *C. muridarum*-specific $CD4^+$ Th1-cell clones, but not Th2-cell clones, protected nude mice against infection with *C. muridarum* (3, 4). $CD8^+$ T cells are recruited to sites of infection and are capable of producing IFN-γ in a chlamydial antigen-specific fashion (4). While certain clones of $CD8^+$ T cells have been shown to be protective, mice deficient in the MHC class I pathway or $CD8^+$ T cells, or depleted of the $CD8^+$ T cell compartment do not display a marked inability to clear the primary genital chlamydial infection (4). Therefore, the role of $CD8^+$ T cells in anti-chlamydial immunity remains to be clarified. The production of anti-*Chlamydia* antibodies is induced during the infection (6). However, mice deficient in B-cells are capable of resolving the primary genital tract infection comparable to wild type animals (6). Although the role of antibodies in primary infections remains to be clarified, an important role for antibody has been described in immunity to secondary infection (6).

Dendritic cells play a key role in the recognition of infection and the induction of a protective Th1 response. Infection with *C. muridarum* has been shown to stimulate DCs to produce IL-12 (a cytokine that polarizes immune responses to Th1-type responses) and CXCL10

(a chemokine that recruits T cells), and to express CCR7, a chemokine receptor that is required for the migration of DCs to local lymph nodes. Furthermore, DCs pulsed with live *C. muridarum* have been shown to be produce a protective immune response comparable to that produced by a primary infection (4).

The inflammatory response to *Chlamydia* infection of the upper genital tract has been reported to contribute to the pathological sequelae (7). Various pro-inflammatory cytokines are secreted by epithelial cells upon infection that recruit effector cells and lymphocytes to the site of infection (3). These include CXCL1, CXCL8, CXCL16, granulocyte/monocytes colony-stimulating factor (GM-CSF), IL-1α, IL-6 and, and tumor necrosis factor (TNF). Infected epithelial cells also secrete cytokines including IFN-α and IFN-β that promote the production of IFN-γ (3). While cytokine induction may play a role in polarizing the immune response towards a protective Th1-type response, cytokines such as TNF, IL-1α and IL-6 also have been suggested to be involved in the pathology associated with infection (3, 19). In this regard, mice depleted of TNF-α or IL-6 have no deficiency in their ability to resolve primary infection or resist secondary challenge. Furthermore, infection of TLR2 knock out mice, that had reduced levels of TNF-α, also showed reduced pathology (19).

The list of immune mediators that may play a role in the development of pathology include cytokines, specifically those induced by the activation of TLR2 (7, 19), proteolytic molecules released by neutrophils (7) such as MMP-9 (20), and $CD8^+$ T cells (4). Specifically, in studies with TLR2 knockout mice (7, 19), and where MMP was inhibited, oviduct pathology did not occur in response to intravaginal challenge with *C. muridarum.* O'Connel *et al.* (7) demonstrated that infection with a plasmid-deficient *C. muridarum* mutant that did not stimulate

TLR2-dependent cytokine production resulted in an effective Th1 immune response and no evidence of Th1-immune mediated collateral tissue damage. TLR2-deficient mice do not develop oviduct pathology after chlamydial infection, indicating that TLR2 signaling is directly involved in disease development (7). They also found that TLR2 knockout mice expressed less TNF-α and that TLR2 knockout macrophages expressed lower levels of TLR2 and IL-6 (19). The authors concluded that, in this model of infection, TLR2 is dispensable with respect to resolution of infection, and is solely disadvantageous with regard to development of immunopathology (7).

In 2006, Imtiaz *et al*. (20), showed that the inhibition of matrix metalloproteinases (MMP) protects mice from ascending infection and chronic disease manifestation resulting from *C. muridarum* infection (20). MMP-9 is a proteolytic enzyme that has been postulated to be involved in the tissue dissolution that accompanies upper genital tract infection. A significant source of MMP-9 during infection is the acute inflammatory cell infiltrate (20). While inhibition of MMP did not affect the shedding of viable *Chlamydia* from the lower genital tract, it did prevent the development of hydrosalpinx. The use of one MMP inhibitor prevented the ascension of bacteria to the upper reproductive tract, with that fact being the likely cause of reduced oviduct pathology (20). However, a second MMP inhibitor reduced the development of hydrosalpinx, even with the presence of bacteria in the upper reproductive tract and an incidence of pyosalpinx similar to controls (20). Therefore, it appears that MMP-9 may play a role both in ascent of chlamydial infection, and in induction of pathology locally in the oviductal regions (20). Collectively, given the complex nature of the immune response, a clear understanding of chlamydial infection in different regions of the genital tract is necessary.

Reproductive Biology – Differences Between the Upper and Lower Genital Tract

The mucosal immune system in the female reproductive tract has evolved to meet the unique requirements of dealing with sexually transmitted bacterial and viral pathogens, allogeneic spermatozoa, and the immunologically distinct fetus (21). Furthermore, the immune environment in the reproductive tract is tightly controlled by the level of specific sex hormones, which vary throughout the estrous cycle (21). Failure of the immune system either to rid the reproductive tract of pathogens or to resist attacking allogeneic sperm and fetus significantly compromises procreation as well as the health of the mother (21). Antimicrobial peptides, such as defensins, play a key role in preventing infection of the reproductive tract. Other bactericidal compounds secreted by uterine epithelial cells include SLPI, lactoferrin, and lysozyme (21).

Multiple studies have reported specific differences in anatomy and physiology of different regions of the female reproductive tract. For example, the vaginal-cervical region is lined by squamous epithelial cells, whereas the oviducts are lined by columnar epithelium (22). In the context of genital chlamydial infections, there is evidence to show that the upper and lower regions of the genital tract respond differently to genital infection (22). Specifically, during *C. muridarum* infection, $CD4^+$ T cells are preferentially recruited to the upper genital tract over the lower GT (23). This difference is partly attributed to a chemokine expression profile that differs from the lower genital tract (22). The chemokine CXCL10 (IP-10) was expressed on a wider array of cell types in the upper genital tract than in the lower genital tract, further supporting the concept that chemokine secretion associated with Th1 responses was significantly higher in the upper genital tract, even when the number of bacteria in the oviducts was less than that in the vagina. The vagina is constantly exposed to nonpathogenic organisms and normal

flora, and therefore, the immune response in that area may be specifically repressed to prevent damage from constant inflammation (22). Conversely, the upper reproductive tract is essentially sterile in normal conditions, and may respond to any infection with a high level of chemokine expression to attract Th1 cells to the area (3, 22). Collectively, these results suggest that lymphocyte recruitment may be regulated differently between the upper and lower regions of the genital tract and may influence the clearance of *Chlamydia* from the respective regions of the reproductive tract (23).

Rationale and Objectives

There is an accumulating body of evidence to suggest that host immunity may be differentially regulated in different regions of the female reproductive tract (22, 23). However, most studies of *Chlamydia* infection using animal models utilize the quantification of bacterial numbers from vaginal swabs to characterize infection (5, 6, 9, 19). The limitation of this method is that it only represents the level of infection in the lower reproductive tract. However, it is known that *Chlamydia* ascend to the upper reproductive tract where they trigger an immune response that leads to the development of pathology. Given that the upper reproductive tract may differ substantially from the lower reproductive tract in its architecture and immune response, the data from the lower reproductive tract alone may not provide an accurate representation of ascent and kinetics of infection in the upper reproductive tract. Previous studies that sought to characterize the level of infection in the upper genital tract vary widely in the technique used and in the sections sampled. One study collected uterine lavage fluid with the oviducts/ovaries being removed and not included in the analysis (24), while others used tissue homogenates of upper genital tract tissue but made no distinction between right and left sides of the reproductive tract or between the different regions of the upper reproductive tract (9). Additionally, the sensitivity of detection by tissue homogenate for this group was lower than that of vaginal swabbing (9). We performed this study in order to understand the kinetics of ascent and infection in the upper genital tract using the highly sensitive method of real-time PCR. The vagina, and right and left oviducts and ovaries (designated oviducts in this study) were assayed at 7 time points during the first 30 days after challenge (Fig. 1). Additionally, we assayed the bacterial numbers in the cervix, lower uterine horn, and upper uterine horn, at 3 time points

during the first 30 days after infection (Fig. 1). Furthermore, right and left sides of the uterine horns, and oviducts/ovaries were assayed individually. To our knowledge, this is the first time that bacterial numbers have been evaluated in these defined regions of the reproductive tract. By performing quantitative real-time PCR on DNA extracted from these tissue sections, we sought to gain a comprehensive understanding of the ascent of bacteria and kinetics of infection in the upper reproductive tract, and to validate a method of detection that is reliable, sensitive, and independent of the ability to culture viable bacteria. Collectively, these analyses should contribute to the understanding of chlamydial genital tract infections.

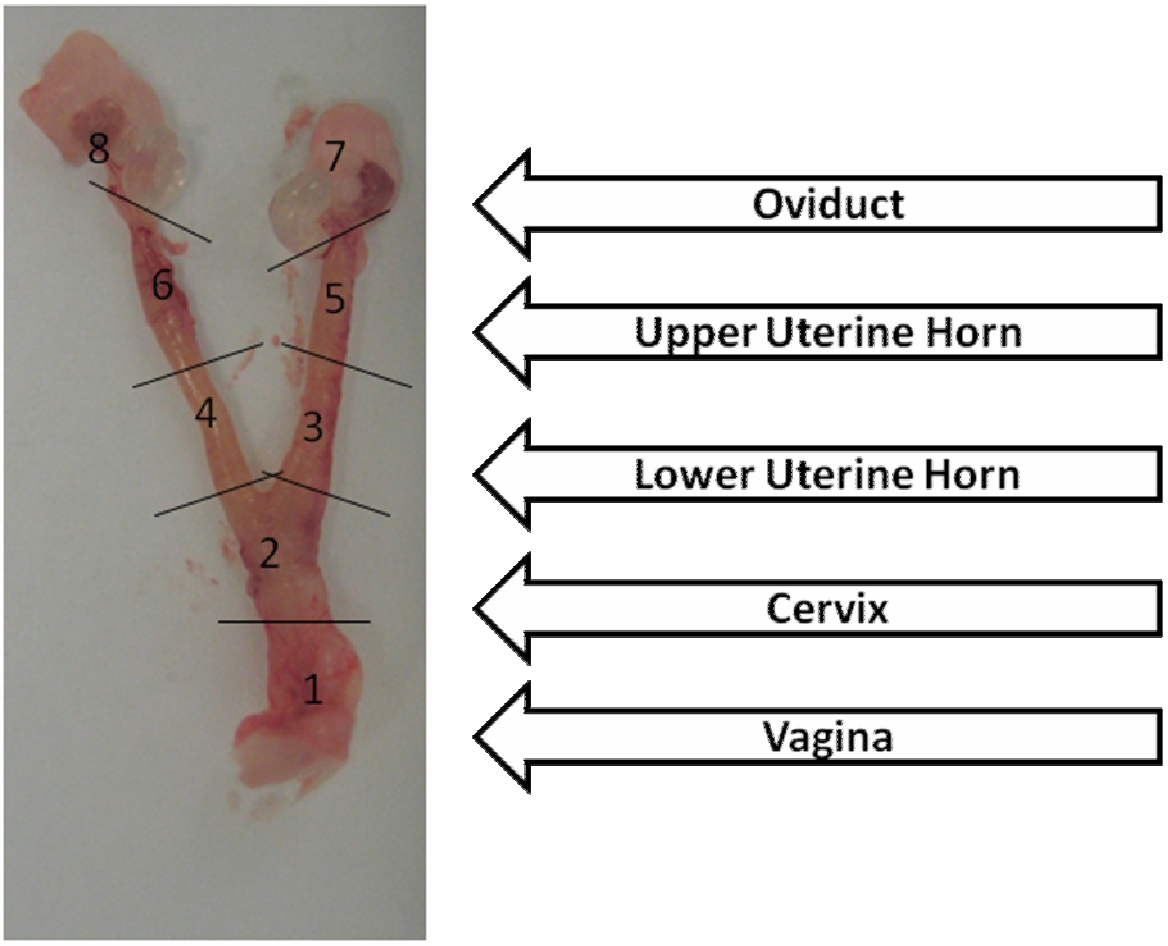

Figure 1. Defined regions of the reproductive tract in which the course of infection was analyzed. This figure visually depicts the tissue regions that were isolated for analysis by real-time PCR.

MATERIALS AND METHODS

Bacteria

C. muridarum was grown on confluent HeLa cell monolayers as described previously. Cells were lysed using a sonicator and elementary bodies purified on Renograffin gradients. Aliquots of bacteria were stored at -80°C in sucrose-phosphate-glutamine buffer (18).

Mice

Four to 6-wk-old female BALB/c mice were purchased from the National Cancer Institute (Bethesda, MD). Mice were housed and bred at the University of Texas at San Antonio. Animal care and experimental procedures were performed in compliance with the Institutional Animal Care and Use Committee (IACUC) guidelines.

Intravaginal Challenge

Mice were inoculated i.vag. with approximately $5x10^4$ inclusion forming units (IFUs) of *C. muridarum* in 5 µl of sterile sucrose phosphate buffer (SPG). At 10 and 3 days prior to challenge, mice received a subcutaneous injection of 2.5 mg of Depo-Provera dissolved in 100 µl of sterile PBS (Pharmacia & Upjohn Co, New York City, NY). The purpose of Depo-Provera injection is to synchronize the estrous cycles of the animals and make all animals equally receptive to infection.

Bacterial Shedding

Vaginal swab material collected at the indicated days after challenge was plated onto HeLa cell monolayers as described previously (25). Briefly, following incubation for 24-28 hours, cells were fixed with 2% paraformaldehyde. Chlamydial inclusions were probed using a polyclonal rabbit anti-*Chlamydia* antibody and goat anti-rabbit Ig secondary antibody conjugated to FITC (Sigma, St. Louis, MO) plus Hoescht nuclear stain, and counted using a Zeiss Axioskop microscope. The average number of inclusions in ten 40X fields (or the number of inclusions on the entire coverslip, whichever was more representative) was calculated for each animal and the data was expressed as the average number of IFUs per animal group.

DNA Isolation and Quantitative Real-Time PCR

Total DNA was obtained from snap frozen reproductive tract sections using the High Pure PCR Template Preparation Kit (Roche Diagnostics, Indianapolis, IN). The manufacturer's instructions were modified to obtain the highest level of DNA extraction. Modifications included the grinding of tissue samples prior to adding any reagents, and the addition of 40 µl of collagenase (from *Clostridium histolyticum*, Type IV) (Sigma-Aldrich, St. Louis, MO) at a concentration of 10 mg/ml prior to overnight incubation of samples. Real-time quantitative PCR was performed with a DyNAmo SYBR Green qPCR Kit (New England BioLabs, Ipswich, MA) using a DNA Engine Opticon 2 continuous fluorescence detection system and Opticon Monitor Software 2.02 (MJ Research, Waltham, MA). Sense and antisense primers used were as follows: MOMP (chlamydial major outer membrane protein) 5' - GCC GTT TTG GGT TCT GCT T - 3' (24) and 5' - CGT CAA TCA TAA GGC TTG GTT CA - 3'; β-actin, 5' – CAA GTC ATC

ACT ATT GGC AAC GA – 3' and 5' – CCA AGA AGG AAG GCT GGA AAA – 3'. Real-time PCR conditions were as follows: 10 s of denaturation at 95 ^{o}C, 20 s of primer annealing at 56 ^{o}C, and 30 s of elongation at 72 ^{o}C for 40 cycles. Quantification was carried out by monitoring the fluorescent DNA binding dye SYBR Green at the end of each elongation cycle at 76^{o}, 78^{o}, and 81 ^{o}C. Absolute quantification was carried out by including internal standards into each real-time PCR run. Standard curves were created by extracting DNA from known quantities of *Chlamydia* elementary bodies and J774 cells and performing quantitative real-time PCR using the same method as that used for the samples. Opticon monitor software was used to calculate the number of *Chlamydia* genomes and mouse genomes based on the standard curves. As shown in Figure 2A, the number of mouse cells in each tissue sampled varied across the samples assayed. In order to account for this variation, as well as any variation in experimental efficiency between time points, the total number of chlamydial genomes was normalized to the number of mouse cells present in the tissue sample. Normalization of the data resulted in a trend of infection (Fig. 2C) very similar to that of the absolute number of chlamydial genomes (Fig. 2B), and this held true across all regions of the genital tract. Therefore, data was expressed as relative *Chlamydia* IFUs per 10^{7} mouse cells.

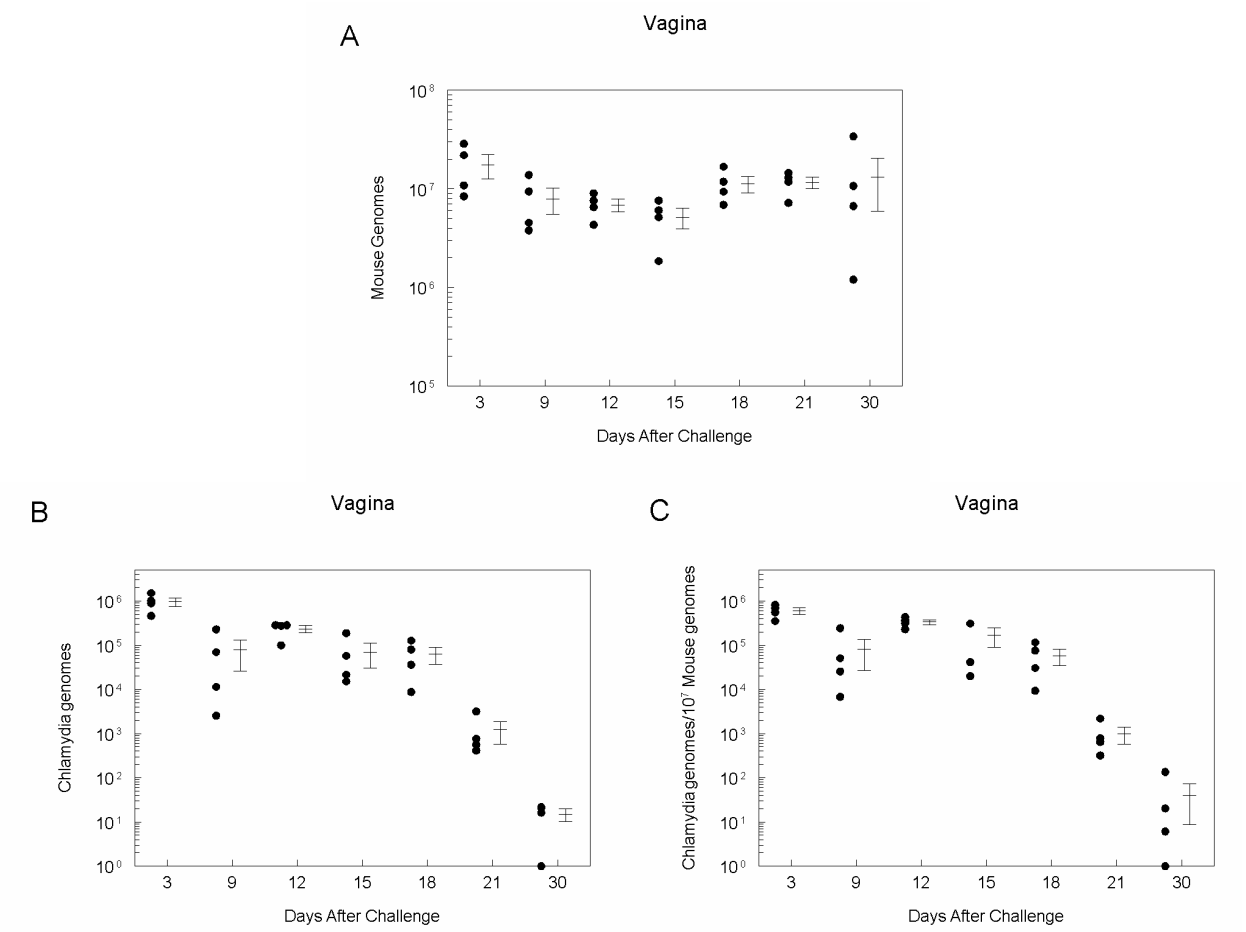

Figure 2. Normalization of the absolute number of chlamydial genomes to the number of mouse cells present in a tissue sample accounted for any variation due to experimental efficiency without affecting the observed trend of infection. (A) The trend of infection in the vagina expressed in the total number of chlamydial genomes recovered (B) The total number of mouse genomes recovered from tissue samples at each time point (3) The trend of infection expressed as *Chlamydia* genomes/10^7 Mouse genomes. The ability to normalize the data without affecting the trend of infection held true for all tissue regions analyzed.

RESULTS

I. Quantitative real-time PCR is a viable and sensitive method for the detection of *Chlamydia* genomes from reproductive tract tissues.

DNA extraction was performed using the Roche High Pure PCR Template Preparation Kit on serial ten-fold dilutions of known numbers of *Chlamydia* EBs (as determined previously by plating on HeLa cells and immunofluorescent staining) and murine macrophages (J774 cells) (as determined by counting with a hemocytometer). The extracted DNA from these samples was then assayed by real-time PCR. The melting temperature for the amplicons consisted of a single peak (79.2^{o}C for chlamydial MOMP-Fig. 3A, and 78.2^{o}C for murine β-actin-Fig. 4A), and the same peak was maintained for all samples amplified with these primers. Additionally, the amplification curves for the known ten-fold serially diluted samples showed clear separation from one another (Fig. 3B and Fig. 4B). In order to produce a standard curve from which we could quantify unknowns, the C(t) value was plotted against the log value of the initial number of cells that underwent DNA extraction (the number of chlamydial EBs and J774 cells). The standard curves had r^2 values of 0.965 and 1.0 for chlamydial MOMP and β-actin primers, respectively (Fig. 3C and Fig. 4C). Chlamydial genomes in the range of 10-10^6 and mouse β-actin genomes in the range of 10^4-10^6 could be readily detected. This data validates the use of real-time PCR for detection of chlamydial and mouse genomes from total extracted DNA.

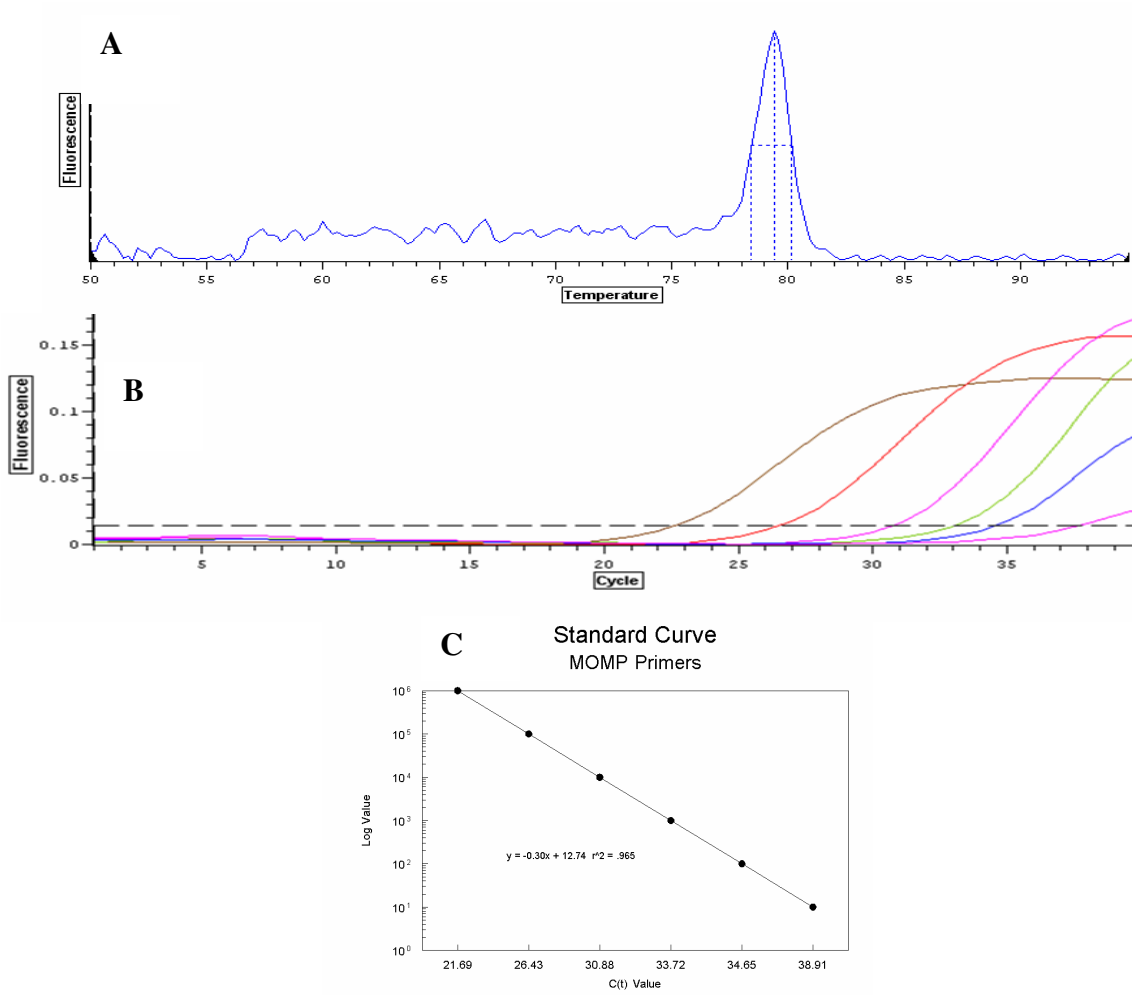

Figure 3. Extraction of DNA and real-time PCR is a precise and sensitive way to quantify *Chlamydia* genomes. (A) A single peak for the melting temperature of the amplified *Chlamydial* DNA verifies the specificity of the primers. (B) Serial dilutions of DNA extracted from *Chlamdyia* EBs resulted in real-time PCR results showing clear separation between the ten-fold serially diluted samples. (C) When the log values of the number of EBs from which DNA was extracted were graphed against the C(t) values, a standard curve with an r^2 value of 0.965 was produced, showing the precision and sensitivity of both DNA extraction and real-time PCR.

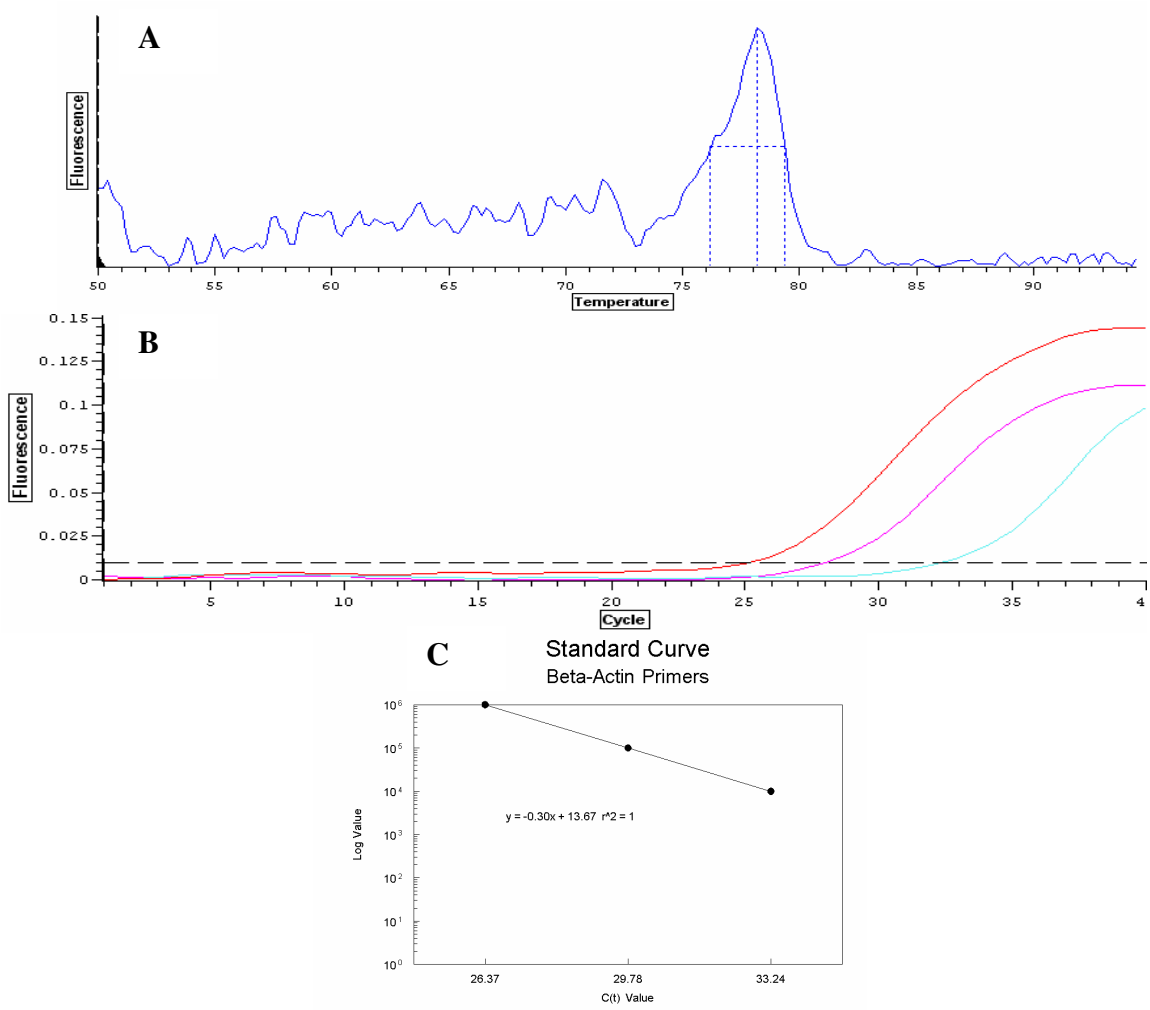

Figure 4. Extraction of DNA and real-time PCR is a precise and sensitive way to quantify the number of mouse genomes in a tissue sample. (A) A single peak for the melting temperature of the amplified murine DNA verifies the specificity of the primers. (B) Serial dilutions of DNA extracted from J774 cells resulted in real-time PCR results showing separation between the ten-fold serially diluted samples. (C) When the log values of the number of EBs from which DNA was extracted were graphed against the C(t) values, a standard curve with an r^2 value of 1.0 was produced, showing the precision and sensitivity of both DNA extraction and real-time PCR.

II. Course of chlamydial infection as determined by vaginal swabbing (Fig. 5).

Following Depo-Progesterone treatment, BALB/c mice (*n*=6) were challenged i. vag. with approximately 5 X 10^4 IFU of *C. muridarum*. The highest level of bacteria was present 3 days after challenge (5.1E+3 ± 1.9E+3). On day 9, the level of bacteria had decreased (4.8E+2 ± 1.1E+2). At 12 and 15 days after challenge, the numbers of bacteria recovered were slightly higher (8.8E+2 ± 2.8E+2 and 1.7E+3 ± 2.7E+2 respectively). The number of bacteria decreased from day 15 to day 18 (4.8E+2 ± 2.2E+2). At 21 days after challenge, viable *Chlamydia* could not be recovered from 50% of the animals, while the remainder continued to shed low levels of bacteria (1.7E+2 ± 1.4E+2). At 30 days after challenge, no viable *Chlamydia* could be detected by vaginal swabbing. This data indicates a trend in which the numbers of bacteria remain high through day 15 before showing a large decrease in bacterial burden by day 18 and eventual clearance by 30 days after challenge.

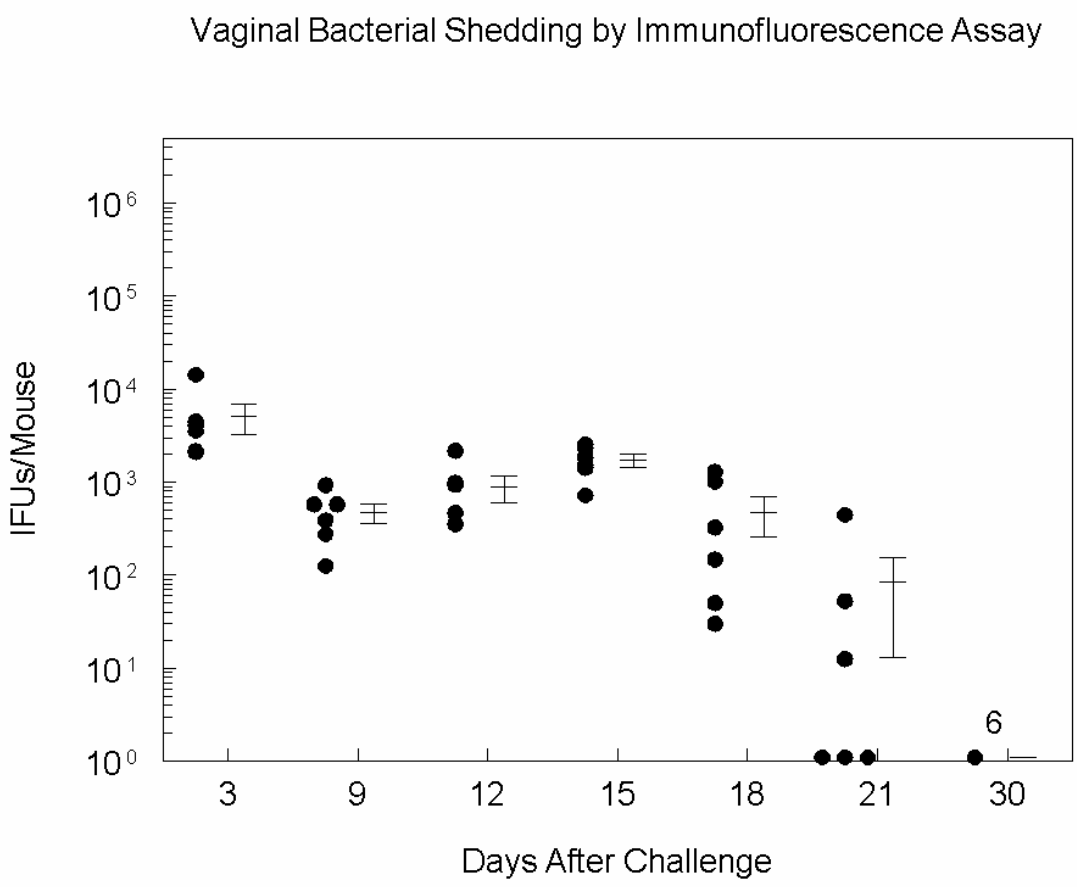

Figure 5. Resolution of infection from the vagina as indicated by vaginal swabbing and immunofluorescence assay. Following Depo-Progesterone treatment, mice (*n*=6) were challenged i.vag with approximately 5 X 10^4 IFU of *C. muridarum* and bacterial shedding was monitored by vaginal swabbing at three day intervals. Each animal is represented by a separate marker. Values indicated on the x-axis shown that no viable *Chlamydia* were detected. The number on the x-axis indicates that all 6 animals were free of detectable *Chlamydia.*

III. Comparison of chlamydial burden in the vagina (lower genital tract) and oviducts (upper genital tract).

BALB/c mice (*n*=4) were challenged i.n. with approximately 5 X 10^4 IFU of *C. muridarum*. The course of infection in the lower (vagina) and upper (oviducts) genital tract was analyzed in respective tissue samples collected from euthanized mice at seven indicated time points within the first 30 days after challenge.

Vagina: As shown in Figure 6, the bacterial load in the vagina was highest 3 days after challenge (6.0E+5 ± 1.0E+5). On day 9, high numbers of *Chlamydia* were still present (8.2E+4 ± 5.4E+4) in the vagina, although a drop in bacterial numbers by about one log was seen. On day 12, the number of *Chlamydia* remained high (3.4E+5 ± 4.3E+4), with a small decline from day 3 being apparent. Thereafter, an approximately 0.5 log decrease was observed between each time point for days 12(3.4E+5 ± 4.3E+4), 15 (1.7E+5 ± 8.1E+4), and 18 (5.8E+4 ± 2.4E+4). This was followed by a decrease of about 2 logs between days 18 and 21 (9.8E+2 ± 4.1E+3). On day 30 after challenge, the mice demonstrated a trend towards resolution of infection with chlamydial numbers being below the level of detection (less than 10 genomes) in one mouse, and minimal but detectable numbers (6 to 125 organisms per 10^7 mouse genomes) in the other three animals. In these analyses, real-time PCR for the vaginal section appeared to be a more sensitive technique when compared to vaginal swabbing (Fig. 5) for detection of chlamydial organisms.

Right Oviduct: As shown in Figure 7, bacteria can be found in the right oviduct of infected mice as early as 3 days post challenge (2.0E+3 ± 1.3E+3). At 9 days after challenge, the number of bacteria had increased by about 2 logs (6.1E+4 ± 2.1E+4), suggesting an ascending infection. On days 12 and 15 after challenge, high numbers of bacteria (5.3E+3 ± 3.5E+3 and

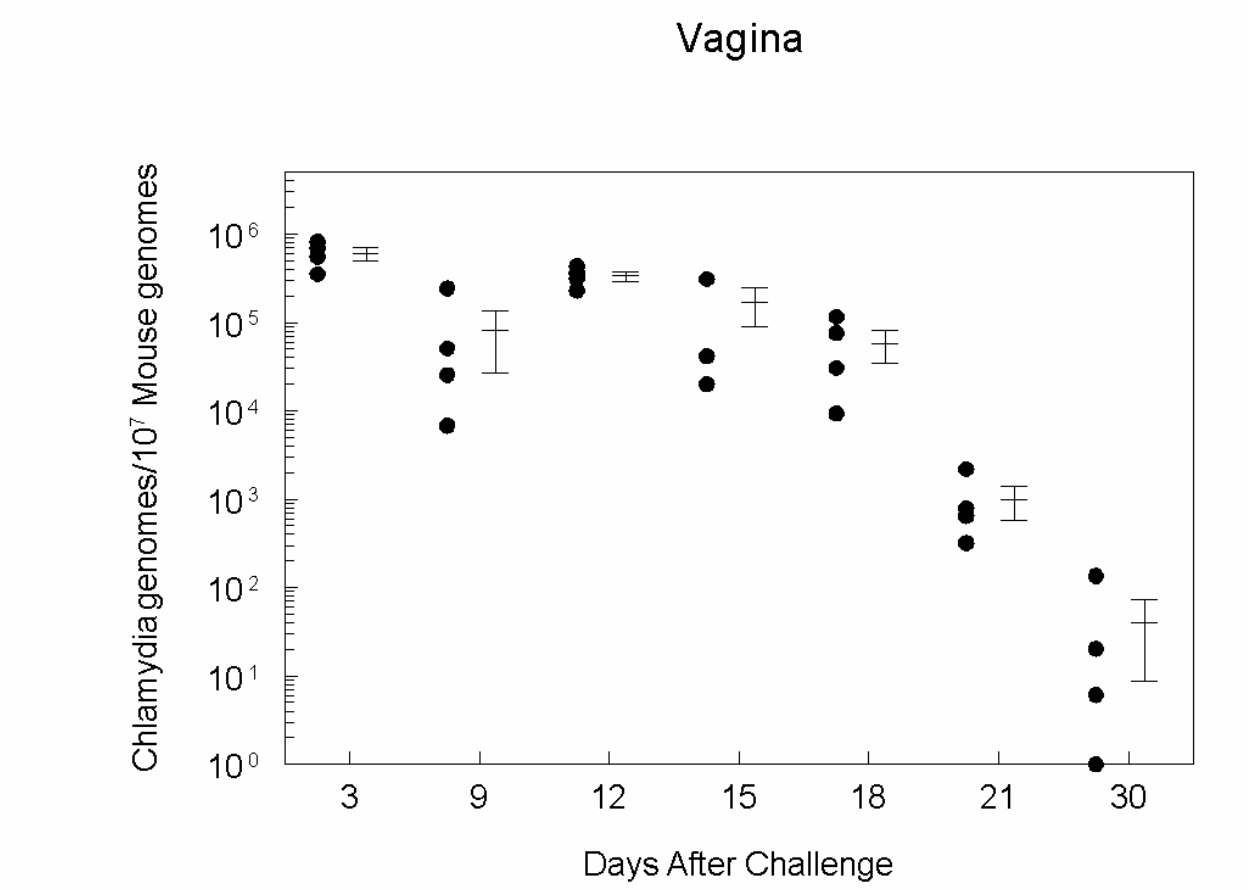

Figure 6. Course of infection in vaginal tissue as indicated by real-time PCR. Following Depo-Progesterone treatment, mice (4 per group/time point) were challenged i.vag with approximately 5 X 10^4 IFUs of *C. muridarum*. At the indicated time periods after challenge, mice were euthanized and vaginal samples were obtained, DNA extracted, and real-time PCR performed. Data is represented as the number of *Chlamydia* genomes per 10^7 mouse genomes present in each tissue section sampled. Samples that lay on the x-axis indicate that the amount of amplicon was too low to be accurately quantified.

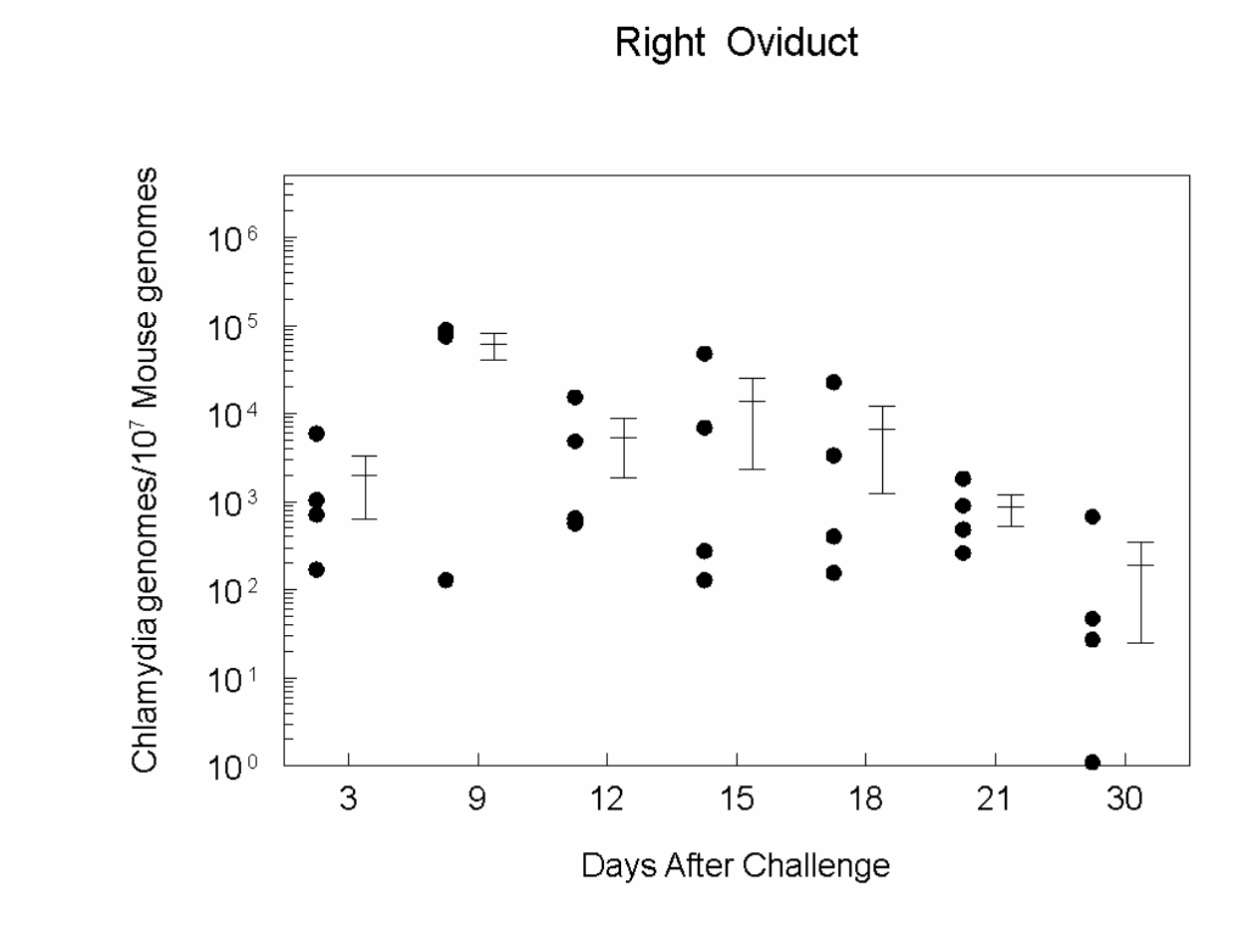

Figure 7. Course of infection in the right oviduct as indicated by real-time PCR. Following Depo-Progesterone treatment, mice (4 per group/time point) were challenged i.vag with approximately 5 X 10^4 IFUs of *C. muridarum*. At the indicated time periods after challenge, mice were euthanized and the right oviducts were obtained, DNA extracted, and real-time PCR performed. Data is represented as the number of *Chlamydia* genomes per 10^7 genomes present in each tissue section sampled. Samples that lay on the x-axis indicate that the amount of amplicon was too low to be accurately quantified.

1.4E+4 ± 1.2E+4, respectively) were present, albeit the numbers being lower than on day 9, suggesting an ongoing infection. After day 15, the number of bacteria began to decrease (day 18: 6.7E+3 ± 5.4E+3 and day 21: 8.6E+2 ± 3.4E+2), indicating the onset of chlamydial clearance. At day 30 after challenge, one mouse had cleared the infection of detectable *Chlamydia* genomes, while the remaining animals had low numbers of *Chlamydia*. In a previous experiment (Fig. 9), 100% of challenged animals had cleared the infection from the right oviduct by day 30 after challenge.

Left Oviduct: The bacterial levels in the left oviduct at day 3 (7.2E+3 ± 3.7E+3) are slightly higher than in the right oviduct (Fig. 8). At 9 days after challenge, there was approximately a 0.5 log increase in the number of bacteria (2.5E+4 ± 1.1E+4). The number of bacteria on day 12 (2.6E+4 ± 1.2E+4) was comparable to that seen on day 9. A decrease in bacterial numbers of about 1 log was seen between days 12 and 15 (3.4E+3 ± 2.0E+3), followed by only a slight decrease in numbers between days 15 and 18 (2.1E+3 ± 1.4E+3), and between days 18 and 21 (1.8+E3 ± 3.6+E2). At 30 days after challenge, the level of infection in all mice was below the detection limits of our assay (10 genomes).

Collectively, the course of chlamydial infection in the vagina and oviducts were generally comparable in that high levels of infection were maintained through day 15, followed by significant decreases in bacterial numbers at or after 18 days leading towards complete resolution of infection at day 30 after challenge. However, in the early phase, the level of infection in the lower genital tract was highest at day 3, whereas in the upper genital tract, the level of infection increased from day 3 and displayed peak levels at day 9 after challenge, which may suggest the ascent of the chlamydial infection.

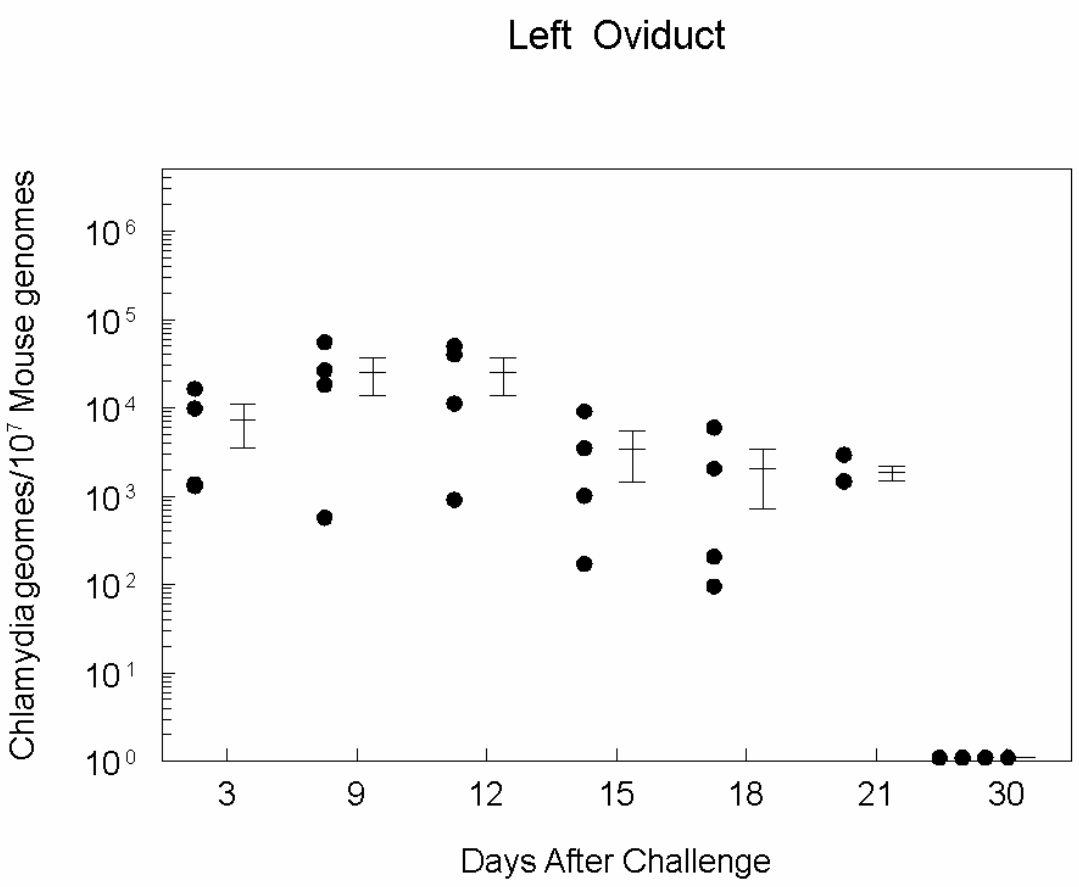

Figure 8. Course of infection in the left oviduct as indicated by real-time PCR. Following Depo-Progesterone treatment, mice (4 per group/time point) were challenged i.vag with approximately 5 X 10^4 IFUs of *C. muridarum*. At the indicated time periods after challenge, mice were euthanized and the left oviducts were obtained, DNA extracted, and real-time PCR performed. Data is represented as the number of *Chlamydia* genomes per 10^7 mouse cells present in each tissue section sampled. Samples that lay on the x-axis indicate that the amount of amplicon was too low to be accurately quantified.

IV. Detailed evaluation of *C. muridarum* presence in defined regions of the murine female reproductive tract.

In a second series of experiments, we evaluated the kinetics of chlamydial infection in defined regions across the entire reproductive tract, including the vagina, cervix, the lower uterine horns, upper uterine horns, and the oviducts, with the right and left sides assayed separately. Bacterial numbers were analyzed at days 3 (early), 18 (mid), and 30 (late) after challenge as described previously.

Vagina: In the vaginal tissue section, bacterial levels were highest at 3 days after challenge (2.0E+6 ± 6.3E+5). The number of *Chlamydia* displayed an approximately 2.5 log reduction by day 18 after challenge (6.4E+3 ± 4.1E+3). At 30 days after challenge, 50% of the animals had cleared the infection to genome levels below our detection limit, while the remainder continued to harbor low numbers of *Chlamydia* genomes (37 ± 21). The pattern of chlamydial burden in the vaginal section on the indicated days in this experiment was comparable to those observed in the earlier experiment (Fig. 9).

Cervix: The chlamydial burden in the cervix also was analyzed on days 3, 18, and 30 after challenge. The overall trend of the course of infection in the cervix (Fig. 10) was similar to that observed in the vagina (Fig. 9), whereas the absolute numbers of Chlamydia were lower than in the vagina. Specifically, the chlamydial burden was highest on day 3 (8.7E+4 ± 8.0E+4), intermediate on day 18 (2.3E+3 ± 1.0E+3), with all mice having cleared the infection by day 30 after challenge.

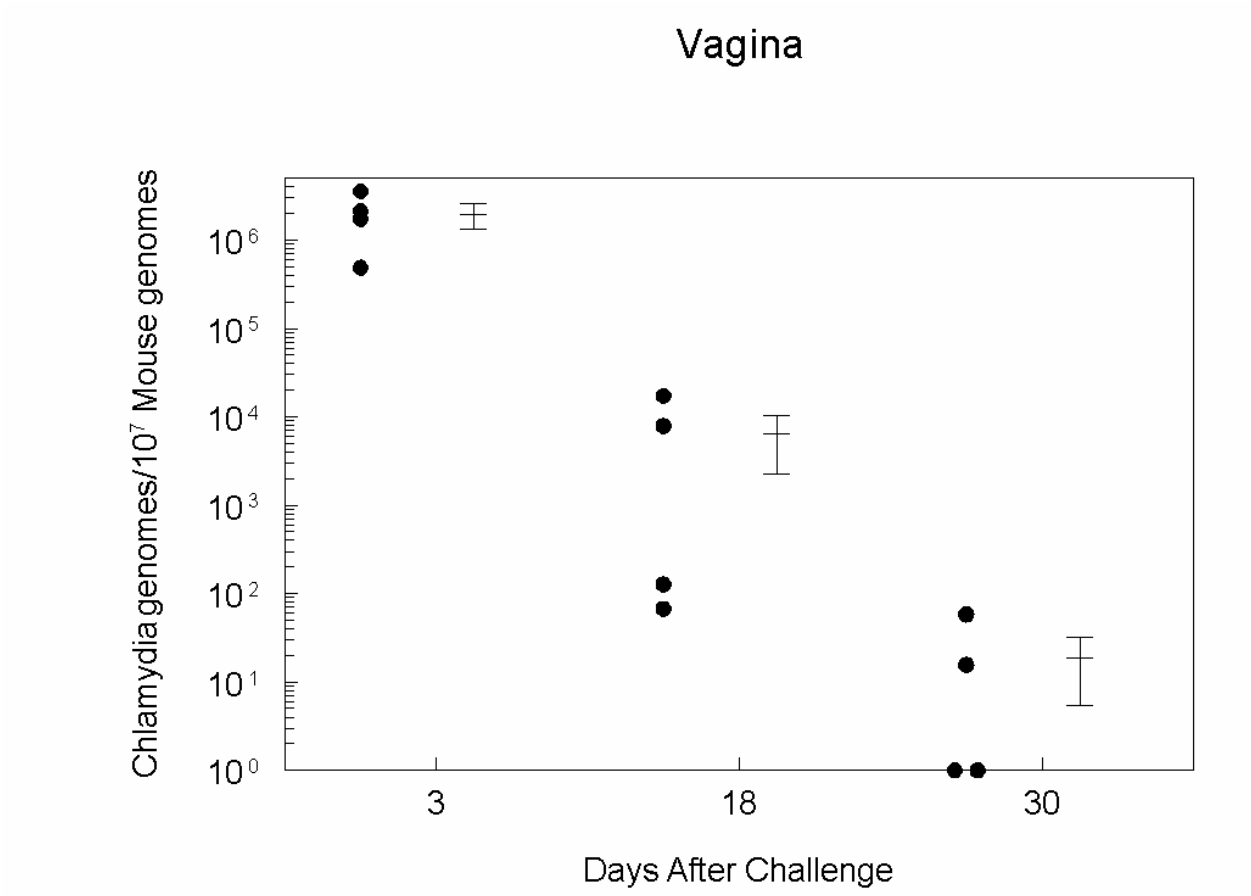

Figure 9. Course of infection in vaginal tissue as indicated by real-time PCR. Following Depo-Progesterone treatment, mice (4 per group/time point) were challenged i.vag with approximately 5 X 10^4 IFUs of *C. muridarum*. At the indicated time periods after challenge, mice were euthanized and the vaginal tissues were obtained, DNA extracted, and real-time PCR performed. Data is represented as the number of *Chlamydia* genomes per 10^7 mouse cells present in each tissue section sampled. Samples that lay on the x-axis indicate that the amount of amplicon was too low to be accurately quantified.

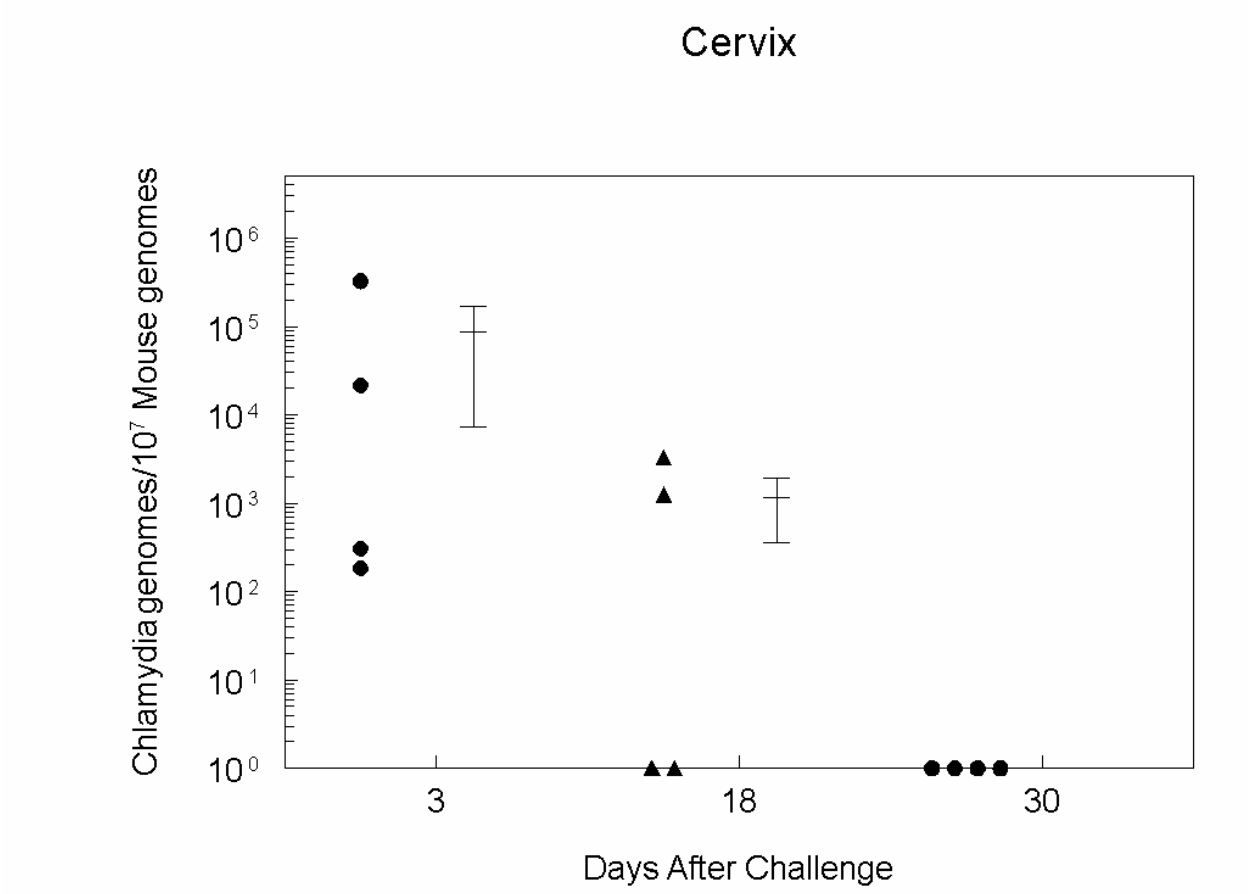

Figure 10. Course of infection in cervical tissue as indicated by real-time PCR. Following Depo-Progesterone treatment, mice (4 per group/time point) were challenged i.vag with approximately 5 X 10^4 IFUs of *C. muridarum*. At the indicated time periods after challenge, mice were euthanized and the tissue of the cervical areas was obtained, DNA extracted, and real-time PCR performed. Data is represented as the number of *Chlamydia* genomes per 10^7 mouse cells present in each tissue section sampled. Samples that lay on the x-axis indicate that the amount of amplicon was too low to be accurately quantified.

Lower Uterine Horns: In the right lower uterine horn (Fig. 11), all infected mice displayed a chlamydial burden on day 3 after challenge (3.8E+2 and 2.7.8E+2). However, chlamydial numbers were low when compared to the vaginal region at the same time-point (Fig. 9). At 18 days after challenge, 50% of infected mice were free of detectable genomes, while the remaining mice continued to harbor detectable *Chlamydia* (2.1E+2 ± 9.7E+1). In the left lower uterine horn (Fig. 12), the chlamydial burden on day 3 after challenge (7.8E+2 ± 4.8E+2) was comparable to that in the right lower uterine horn. On day 18 after challenge, chlamydial burden in 75% of the animals was below detection limits, whereas the remaining animal continued to sustain the infection (2.3E+2). On day 30, 100% of the mice had cleared the infection from both the right and left lower left uterine horns.

Upper Uterine Horns: The pattern of infection in the upper uterine horns differs from that in the lower uterine horns. In the right upper uterine horn (Fig. 13), all infected mice displayed chlamydial burden on day 3 after challenge (1.6E+2 ± 1.4E+2). However, chlamydial numbers were low when compared to the lower uterine horns at the same time-point. At 18 days after challenge, one mouse (25%) was free of detectable genomes, while the remaining animals displayed chlamydial burden (2.1E+3 ± 1.7E+3). In the left upper uterine horn, the chlamydial burden on day 3 after challenge (1.5E+2 ± 4.5E+1) was comparable to that in the right upper uterine horn, and lower than that in the right lower uterine horn at the same time point. On day 18 after challenge, 100% of the animals sustained a level of infection (6.5E+2 ± 2.9E+2). On day 30, 100% of the mice had cleared the infection from both the right and left upper uterine horns.

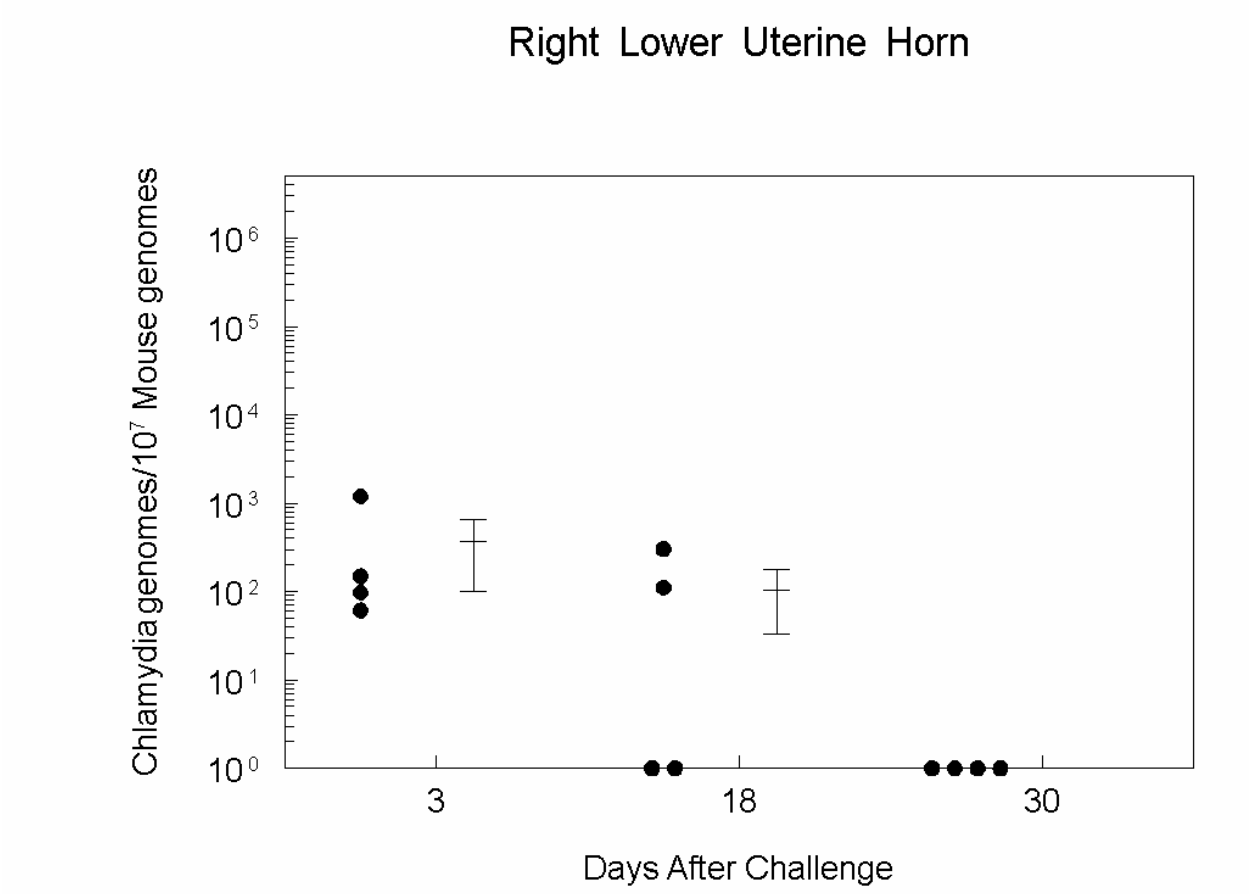

Figure 11. Course of infection in the lower half of the right uterine horn as indicated by real-time PCR. Following Depo-Progesterone treatment, mice (4 per group/time point) were challenged i.vag with approximately 5 X 10^4 IFUs of *C. muridarum*. At the indicated time periods after challenge, mice were euthanized and the right lower uterine horns were obtained, DNA extracted, and real-time PCR performed. Data is represented as the number of *Chlamydia* genomes per 10^7 mouse cells present in each tissue section sampled. Samples that lay on the x-axis indicate that the amount of amplicon was too low to be accurately quantified.

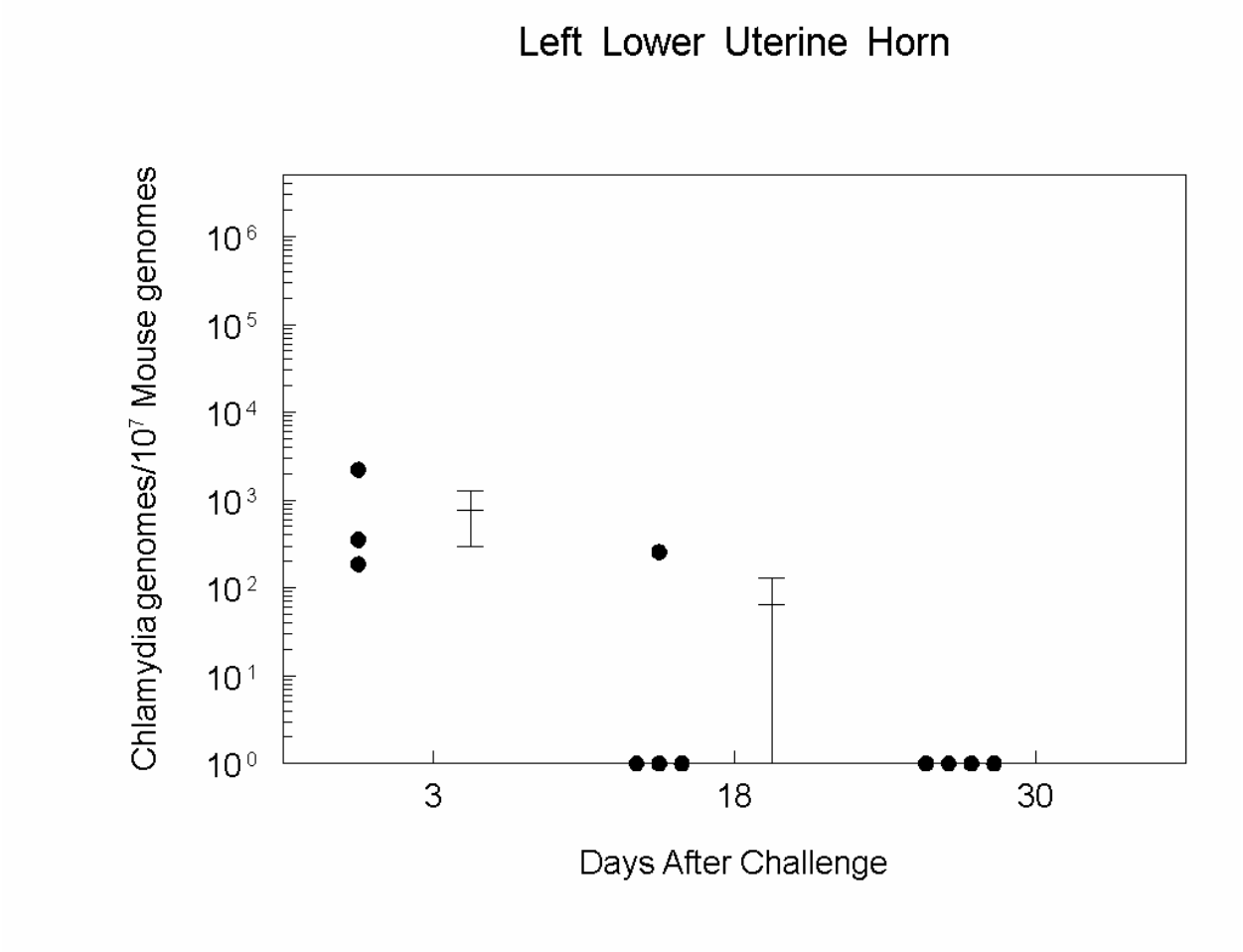

Figure 12. Course of infection in the lower half of the left uterine horn as indicated by real-time PCR. Following Depo-Progesterone treatment, mice (4 per group/time point) were challenged i.vag with approximately 5 X 10^4 IFUs of *C. muridarum*. At the indicated time periods after challenge, mice were euthanized and the left lower uterine horns were obtained, DNA extracted, and real-time PCR performed. Data is represented as the number of *Chlamydia* genomes per 10^7 mouse cells present in each tissue section sampled. Samples that lay on the x-axis indicate that the amount of amplicon was too low to be accurately quantified.

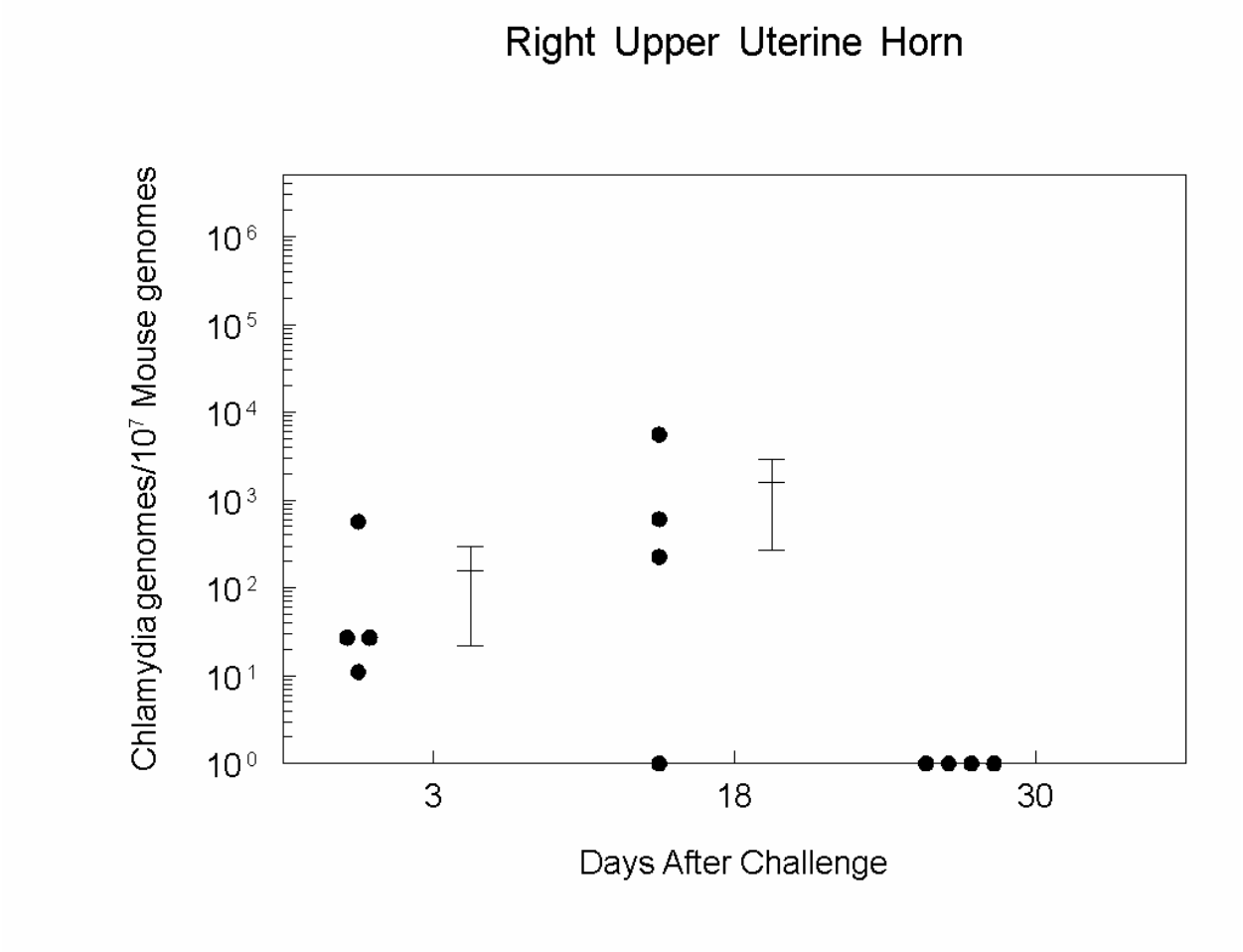

Figure 13. Course of infection in upper half of the right uterine horn as indicated by real-time PCR. Following Depo-Progesterone treatment, mice (4 per group/time point) were challenged i.vag with approximately 5 X 10^4 IFUs of *C. muridarum*. At the indicated time periods after challenge, mice were euthanized and the right upper uterine horns were obtained, DNA extracted, and real-time PCR performed. Data is represented as the number of *Chlamydia* genomes per 10^7 mouse cells present in each tissue section sampled. Samples that lay on the x-axis indicate that the amount of amplicon was too low to be accurately quantified.

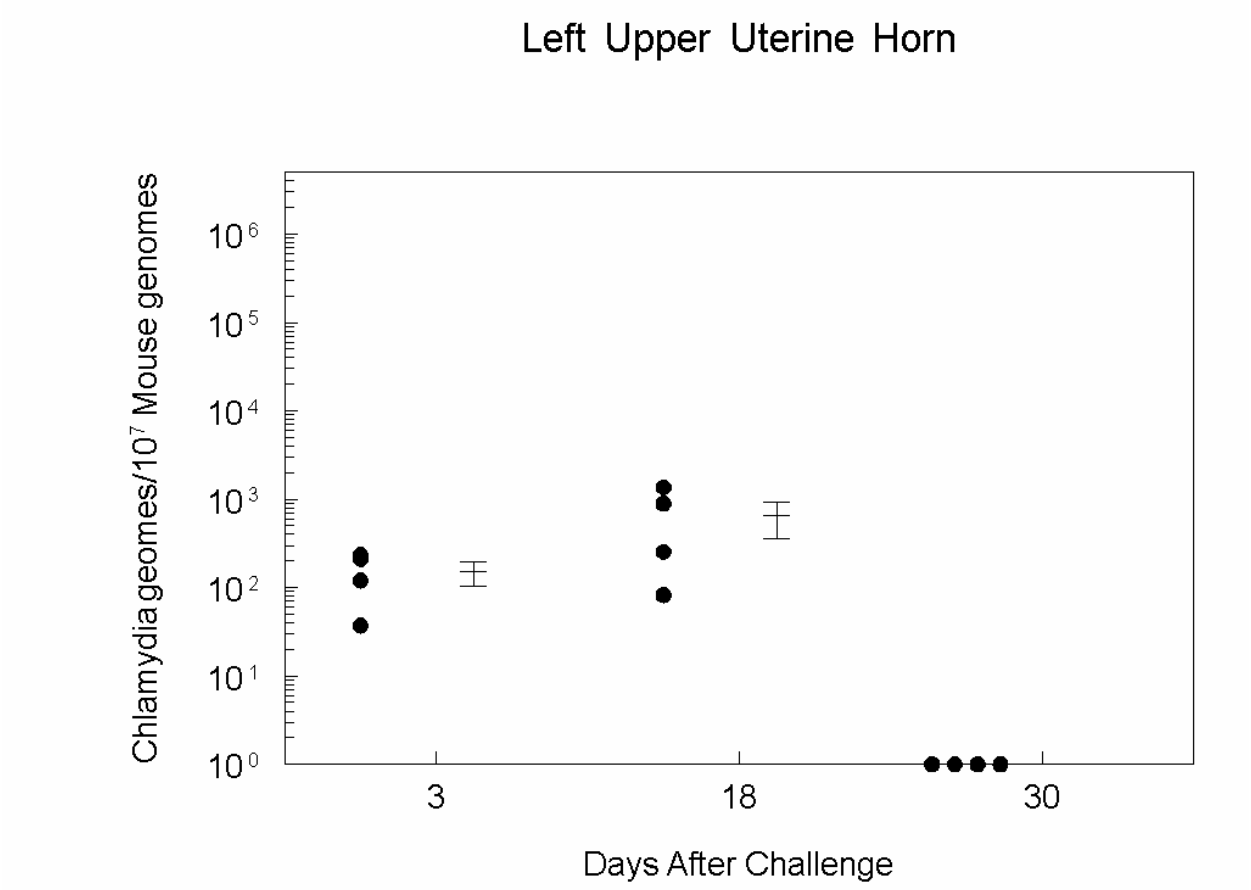

Figure 14. Course of infection in upper half of the left uterine horn as indicated by real-time PCR. Following Depo-Progesterone treatment, mice (4 per group/time point) were challenged i.vag with approximately 5 X 10^4 IFUs of *C. muridarum*. At the indicated time periods after challenge, mice were euthanized and the left upper uterine horns were obtained, DNA extracted, and real-time PCR performed. Data is represented as the number of *Chlamydia* genomes per 10^7 mouse cells present in each tissue section sampled. Samples that lay on the x-axis indicate that the amount of amplicon was too low to be accurately quantified.

Oviducts: The chlamydial burdens in the left (Fig. 15) and right oviducts (Fig. 16) were high on day 3 after challenge (Left: 1.0E+3 ± 4.8E+2; Right: 2.4E+3 ± 2.2E+3). The bacterial burden on day 18 (Left: 1.6E+3 ± 1.4E+3; Right: 4.1E+3 ± 3.1E+3) was somewhat higher, but not significantly, when compared to day 3 after challenge. The infection had been cleared from both the right and left oviducts by day 30 after challenge. These results were comparable to the trends observed in the previously described experiment within these tissue regions.

Course of Ascending Infection: Collectively, these analyses demonstrate that the kinetics of chlamydial infection in the different regions of the murine female reproductive tract is broadly comparable. However, there were differences in the numbers of chlamydial organisms within the different regions (Fig. 17). Specifically, the vaginal region demonstrated a much greater burden (statistically significant with respect to the cervix) compared to any other tissue region, whereas the cervix had the second greatest burden, albeit not statistically significant than the other sections (except vagina). Furthermore, it appears that the chlamydial burden in the uterine horns was generally lower than other regions. Also, there was a trend towards the presence of greater numbers, although not reaching statistical significance, of *Chlamydia* in the lower uterine horns compared to the upper uterine horns on day 3 after challenge, whereas this trend was reversed on day 18 after challenge. Importantly, there was no aspect of laterality to the infection since chlamydial numbers in the corresponding tissue regions from the right and left sides were closely comparable. Taken together, our analyses have provided a detailed characterization of the kinetics of chlamydial infection in various regions of the murine female reproductive tract at multiple time-periods during infection. The results from this study have

provided new insights into the kinetics of genital chlamydial infection that will serve as a useful platform for future studies in this model.

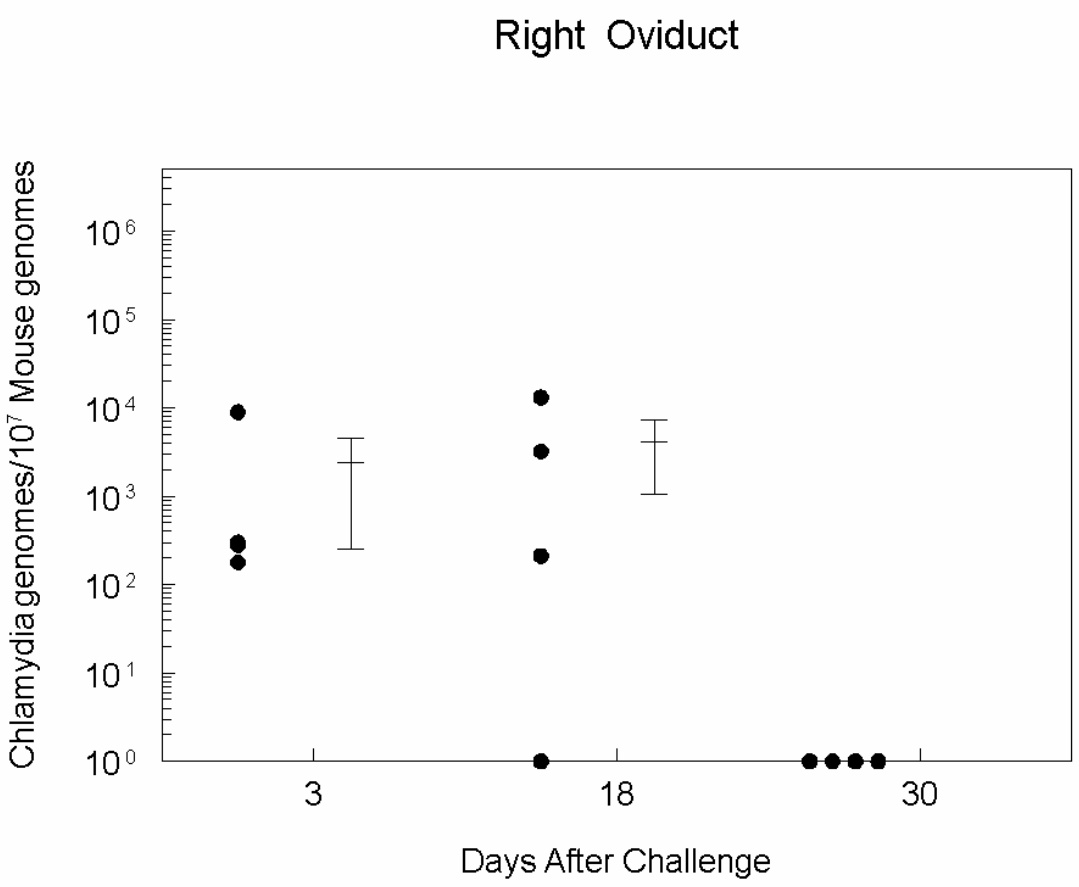

Figure 15. Course of infection in the right oviduct as indicated by real-time PCR. Following Depo-Progesterone treatment, mice (4 per group/time point) were challenged i.vag with approximately 5 X 10^4 IFUs of *C. muridarum*. At the indicated time periods after challenge, mice were euthanized and the right oviducts were obtained, DNA extracted, and real-time PCR performed. Data is represented as the number of *Chlamydia* genomes per 10^7 mouse cells present in each tissue section sampled. Samples that lay on the x-axis indicate that the amount of amplicon was too low to be accurately quantified.

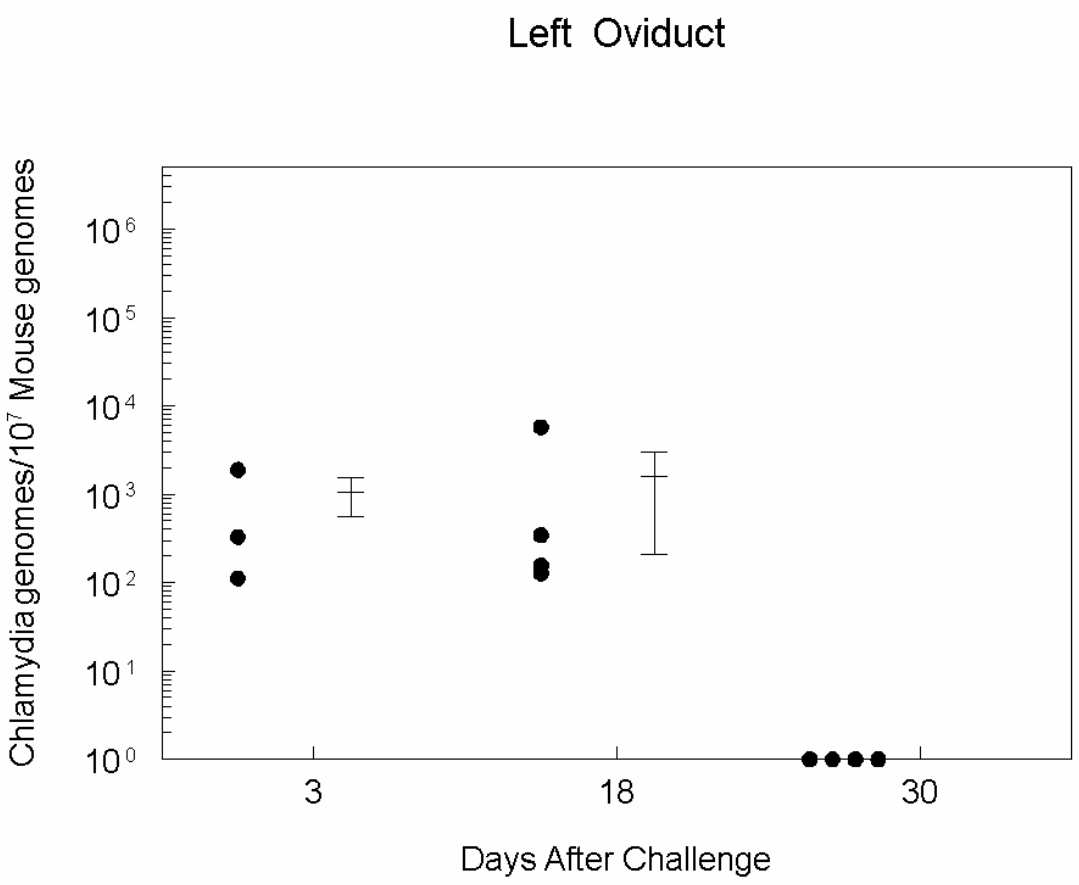

Figure 16. Course of infection in left oviduct as indicated by real-time PCR. Following Depo-Progesterone treatment, mice (4 per group/time point) were challenged i.vag with approximately 5 X 10^4 IFUs of *C. muridarum*. At the indicated time periods after challenge, mice were euthanized and the left oviducts were obtained, DNA extracted, and real-time PCR performed. Data is represented as the number of *Chlamydia* genomes per 10^7 mouse cells present in each tissue section sampled. Samples that lay on the x-axis indicate that the amount of amplicon was too low to be accurately quantified.

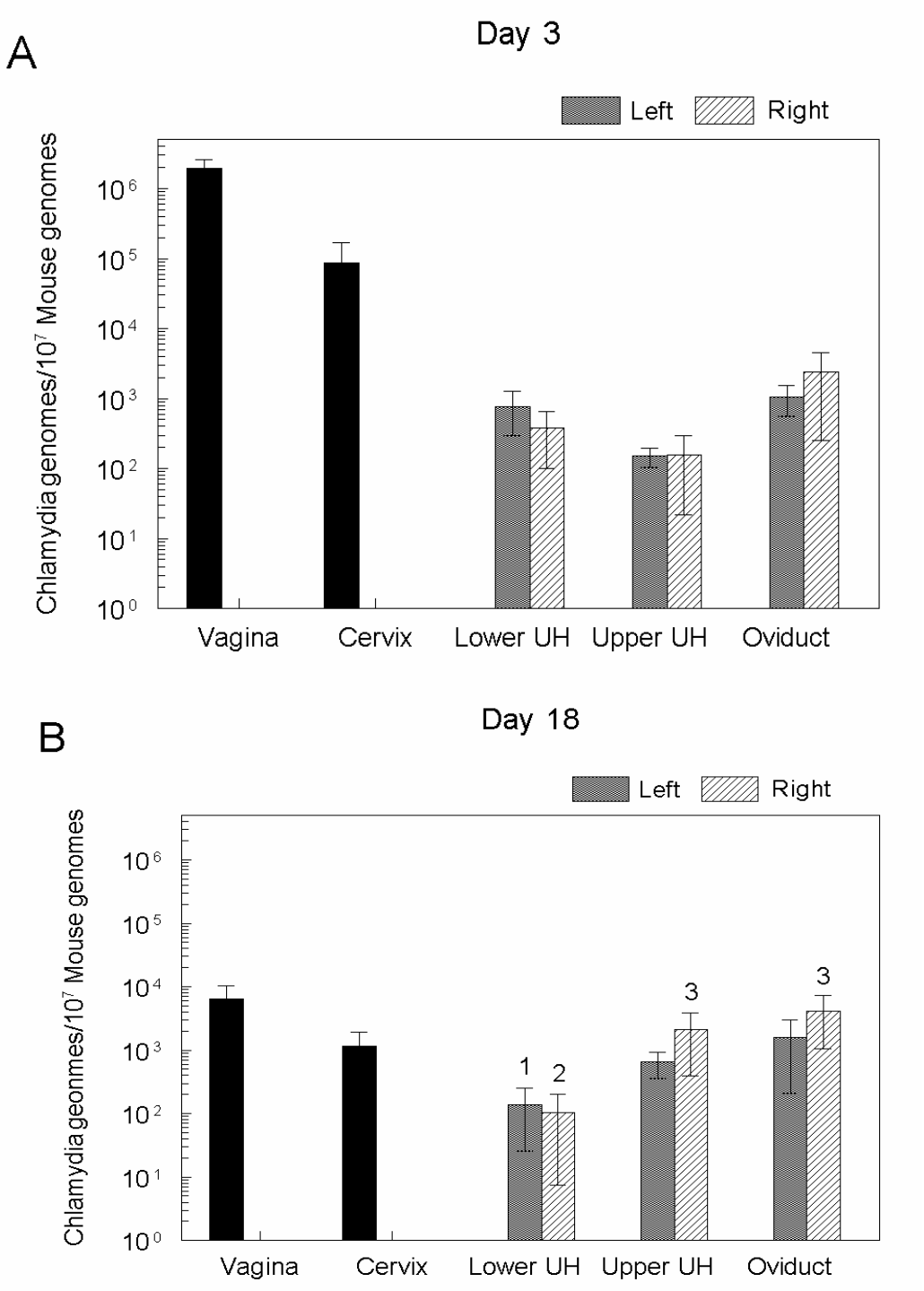
A
Day 3
Left
Right
Chlamydia genomes/10^7 Mouse genomes
10^6
10^5
10^4
10^3
10^2
10^1
10^0
Vagina
Cervix
Lower UH
Upper UH
Oviduct
B
Day 18
Left
Right
Chlamydia geonmes/10^7 Mouse genomes
1
2
3
3
Vagina
Cervix
Lower UH
Upper UH
Oviduct

Figure 17.

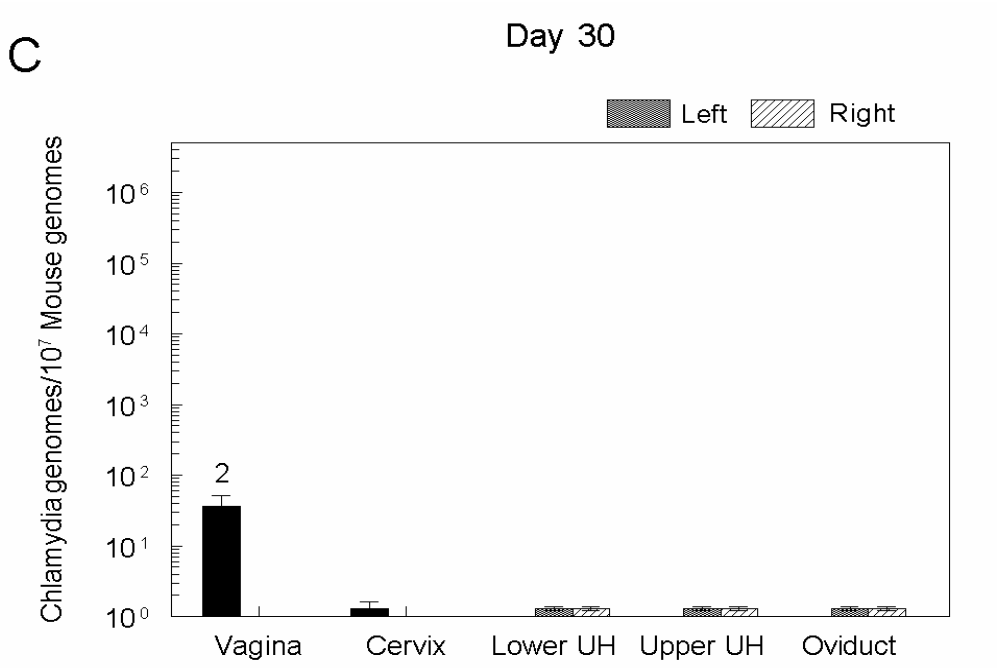

Figure 17 (continued).

Figure 17. Trends of differential distribution of *C. muridarum* throughout the reproductive tract. Following Depo-Progesterone treatment, mice (4 per group/time point) were challenged i.vag with approximately 5 X 10^4 IFUs of *C. muridarum*. At 3 time points after challenge, mice were sacrificed and defined regions of the reproductive tract were isolated, DNA extracted, and real-time PCR performed. Data is represented as the number of *Chlamydia* genomes per 10^7 mouse cells present in each tissue section sampled. LLUH = left lower uterine horn, LUUH = left upper uterine horn, RLUH = right lower uterine horn, RUUH= right upper uterine horn. Numbers above the bars indicate the number of mice with detectable chlamydial genomes whose value(s) are represented on the graph.

DISCUSSION

The anatomy and immunological response to infection in the murine female reproductive tract varies between the lower and upper reproductive tract (22). Genital infection with *C. muridarum* produces an infection that ascends from the vagina, through different regions of the cervix and uterine horns, to the upper reproductive tract. Vaginal infection usually resolves in about 30 days (4), while sequelae in the upper reproductive tract are seen around day 50 after challenge (5). Taken together, these results led us to hypothesize that the kinetics of chlamydial infection varies in different regions within the genital tract. To test this hypothesis, we conducted an extensive characterization of the course of infection in various defined regions throughout the reproductive tract. These analyses provide comprehensive new data which add to the body of evidence from earlier studies of chlamydial infection in the upper reproductive tract which varied widely in the methods of analysis and regions analyzed (9, 24). For example, previous studies have variously assayed the level of infection by lavage fluid (9) or tissue homogenate (24), with no consistent method of analysis between laboratories. Different laboratories also vary in the tissue regions used to asses infection of the upper reproductive tract. One laboratory defined the upper reproductive tract as the uterine horns, but not the oviducts (9), and another vice versa (24), while neither study sought to characterize the left and right sides of the genital tract separately. Our experimental design assessed the course of infection in various defined regions throughout the reproductive tract and included both the use of the conventional method of analysis, vaginal swabbing and immunofluorescence assay, as well as quantitative real-time PCR.

Using the conventional method of vaginal swabbing, we detected high levels of infection by day 3 after challenge, continuing through day 15 with a progressive decline through day 30 after challenge (Fig. 5). This trend is consistent with reports from previous studies using this model (5, 7, 20, 26). In order to characterize the course of infection in the various regions of the reproductive tract, we analyzed the course of infection in the upper and lower reproductive tract at seven time points during the acute phase of infection using quantitative real-time PCR. For these analyses, we studied the vagina (the site of initial infection) and the oviducts (the site of pathological sequelae). In the vagina, the level of bacteria is highest on day 3, with levels remaining high through day 15, followed by a progressive reduction in bacterial numbers through day 30 after challenge (Fig. 6). Although there was some variation, the trend of infection as determined by real-time PCR (Fig. 6) was broadly comparable to that determined by immunofluorescence assay (Fig. 5), indicating that quantitative real-time PCR is a suitable method for the study of the kinetics of chlamydial infection. The number of bacteria detected by real-time PCR was higher than that detected by vaginal swabbing at all time points assayed. Specifically, on days 21 and 30 after challenge, vaginal swabbing indicates that 50% and 100% of animals, respectively, had cleared the infection, whereas real-time PCR detected the presence of chlamydial organisms. This difference in the total number of bacteria recovered suggests that real-time PCR may be a more sensitive method of detection that vaginal swabbing. One reason for the detection of increased numbers may be that real-time PCR is able to detect both live and dead bacteria, while vaginal swabbing is only able to detect viable elementary bodies.

In the right oviduct, we saw a similar trend of high numbers of bacteria from day 3 through 18 before seeing a progressive decline in bacterial numbers through day 30 (Fig. 7). The

trend in the left oviduct is very similar (Fig. 8), with high levels of bacteria from 3 to 12, a decrease in bacterial numbers by day 15, and a large reduction in the bacterial burden from day 21 to 30, with 100% of the animals clearing the infection by 30 days after challenge. The data collected from real-time PCR analysis of the vagina and oviduct tissues suggests that the kinetics of chlamydial infection in the vagina is comparable to those in the oviducts.

Given that the bacteria ascend through the cervix and uterine horns before infecting the oviducts, we assessed the kinetics of chlamydial clearance across all regions of the reproductive tract. Due to the extensive nature of this analysis, we chose to focus on three time points; day 3 (early), day 18 (mid), and day 30 (late) after challenge. The trend of infection in the cervix (Fig. 10) was very similar to that in the vagina (Fig. 9), with the level of infection progressively decreasing from day 3 to 30, but with lower numbers of bacteria overall, as expected of an ascending infection. The same trend of a progressive decline in bacterial burden, with chlamydial numbers less than that seen in the vagina and cervix was observed in both the right and left lower uterine horns (Fig. 11 & 12). The trend of infection shifts between the lower and upper uterine horns, with the level of bacteria present on day 3 after challenge being less than that seen on day 18, followed by a complete clearance of detectable bacteria by 30 days after challenge (Fig. 13 & 14). This trend was common to both the right and left upper uterine horns. In both the right and left oviducts, the number of bacteria present on day 18 was comparable to that on day 3, with complete clearance of detectable bacteria by day 30 after challenge (Fig. 15 & 16).

We then compared the level of infection in the various regions of the reproductive tract relative to each other at days 3, 18, and 30 after challenge (Fig. 17). 3 days after challenge, we

see the highest number of bacteria is present in the vagina, with decreasing numbers as one ascends through the cervix, lower uterine horn, and upper uterine horn. This is what we would expect to see with an ascending infection 3 days after challenge. Surprisingly, the number of bacteria in the oviducts was slightly higher, albeit not statistically significant, than that seen in the upper uterine horns. 18 days after challenge, the level of infection was comparable in the vagina, cervix, upper uterine horns, and oviducts, with all of these regions having a higher level of infection than the lower uterine horns. Comparing the level of infection on day 3 with that seen on day 18, we see that the number of bacteria present has declined in the vagina, cervix, and lower uterine horns, and has increased or remained about the same in the upper uterine horns and oviducts respectively. This may suggest that while the infection is being cleared from the vagina, cervix, and lower uterine horns, the bacteria are still replicating and the level of infection is increasing the upper uterine horns and oviducts, delaying the clearance of bacteria from those regions later than day 18 after challenge. It is also important to note that the bacterial burden in the right and left sides of the reproductive tract was comparable at all time points assayed, as this aspect of chlamydial ascending infection has not been previously described. On 30 days after challenge, the chlamydial organisms had been cleared from all regions of the reproductive tract, with the exception of two mice which exhibited very low numbers of bacteria in the vagina.

Taken together, chlamydial numbers appear to progressively decrease from day 3 to 30 in the vagina, cervix, and lower uterine horns. In the upper uterine horns and oviducts, chlamydial numbers remain high from day 3 to 18 and subsequently decrease from day 18 to 30. We also found that the absolute number of chlamydial organisms differed between regions of the genital tract (Day 3: Vagina > Cervix > Oviducts > Uterine Horns) and that the pattern of bacterial

burden changed during the course of infection (Day 18: Vagina, Cervix, Upper Uterine Horns, Oviducts are comparable and > Lower Uterine Horn). Given that chlamydial organisms were present in all the regions of genital tract as early as day 3 after challenge, further studies to determine the kinetics of bacterial ascent will be needed. Lastly, there were no apparent differences between the right and left side of the genital tract in any defined region.

In summary, the kinetics of chlamydial infection in various regions of the female murine genital tract is broadly comparable, although specific minor differences exist. Therefore, determination of the course of chlamydial infection in the vagina may be broadly reflective of the kinetics of infection in other regions of the genital tract. However, if the absolute numbers of chlamydial organisms at particular time-points is a consideration, a detailed region-specific analysis such as the one described in this study, need to be undertaken. Overall, we now have described a platform that can be used to correlate immunological responses and pathogenesis with the kinetics of chlamydial infection in defined segments of the genital tract. Additionally, this platform can be used to evaluate the efficacy of vaccine regimens on chlamydial clearance within defined segments of the genital tract. Collectively, the results from this study have provided comprehensive information regarding the kinetics of chlamydial infection in various defined regions throughout the female reproductive tract and contributed significant new information to the field of *Chlamydia* research.

REFERENCES

1. **World Health Organization**. 2001. Global Prevalence and Incidence of Selected Curable Sexually Transmitted Infections: Overview and Estimates, *In* . World Health Organization, Geneva.

2. **Centers for Disease Control and Prevention**. 2008. Sexually Transmitted Disease Surveillance, 2006., *In* . U.S. Department of Health and Human Services, Atlanta, GA.

3. **Brunham, R. C. and J. Rey-Ladino**. 2005. Immunology of *Chlamydia* infection: implications for a *Chlamydia trachomatis* vaccine. Nat. Rev. Immunol. **5**:149-161.

4. **Morrison, R. P. and H. D. Caldwell**. 2002. Immunity to murine chlamydial genital infection. Infect. Immun. **70**:2741-2751.

5. **Murthy, A. K., J. P. Chambers, P. A. Meier, G. Zhong, and B. P. Arulanandam**. 2007. Intranasal vaccination with a secreted chlamydial protein enhances resolution of genital *Chlamydia muridarum* infection, protects against oviduct pathology, and is highly dependent upon endogenous gamma interferon production. Infect. Immun. **75**:666-676.

6. **Morrison, S. G. and R. P. Morrison**. 2005. A predominant role for antibody in acquired immunity to chlamydial genital tract reinfection. J. Immunol. **175**:7536-7542.

7. **O'Connell, C. M., R. R. Ingalls, C. W. Andrews, Jr., A. M. Scurlock, and T. Darville**. 2007. Plasmid-deficient *Chlamydia muridarum* fail to induce immune pathology and protect against oviduct disease. J. Immunol. **179**:4027-4034.

8. **Darville, T., C. W. Andrews, Jr., and R. G. Rank**. 2000. Does inhibition of tumor necrosis factor alpha affect chlamydial genital tract infection in mice and guinea pigs? Infect. Immun. **68**:5299-5305.

9. **Maxion, H. K., W. Liu, M. H. Chang, and K. A. Kelly**. 2004. The infecting dose of *Chlamydia muridarum* modulates the innate immune response and ascending infection. Infect. Immun. **72**:6330-6340.

10. **Wira, C. R. and J. V. Fahey**. 2004. The innate immune system: gatekeeper to the female reproductive tract. Immunology **111**:13-15.

11. **Hybiske, K. and R. S. Stephens**. 2007. Mechanisms of *Chlamydia trachomatis* entry into nonphagocytic cells. Infect. Immun. **75**:3925-3934.

12. **Dautry-Varsat, A., A. Subtil, and T. Hackstadt**. 2005. Recent insights into the mechanisms of *Chlamydia* entry. Cell Microbiol. **7**:1714-1722.

13. **Todd, W. J. and H. D. Caldwell**. 1985. The interaction of *Chlamydia trachomatis* with host cells: ultrastructural studies of the mechanism of release of a biovar II strain from HeLa 229 cells. J. Infect. Dis. **151**:1037-1044.

14. **Rank, R. G.** 1994. Animal Model for Urogenital Infections, *In* Methods in Enzymology, vol. 235. Academic Press.

15. **Coers, J., I. Bernstein-Hanley, D. Grotsky, I. Parvanova, J. C. Howard, G. A. Taylor, W. F. Dietrich, and M. N. Starnbach**. 2008. *Chlamydia muridarum* evades

growth restriction by the IFN-gamma-inducible host resistance factor Irgb10. J. Immunol. **180**:6237-6245.

16. **Shah, A. A., J. H. Schripsema, M. T. Imtiaz, I. M. Sigar, J. Kasimos, P. G. Matos, S. Inouye, and K. H. Ramsey**. 2005. Histopathologic changes related to fibrotic oviduct occlusion after genital tract infection of mice with *Chlamydia muridarum*. Sex Transm. Dis. **32**:49-56.

17. **Kim, S. K., M. Angevine, K. Demick, L. Ortiz, R. Rudersdorf, D. Watkins, and R. DeMars**. 1999. Induction of HLA class I-restricted $CD8^+$ CTLs specific for the major outer membrane protein of *Chlamydia trachomatis* in human genital tract infections. J. Immunol. **162**:6855-6866.

18. **Li, W., A. K. Murthy, M. N. Guentzel, J. Seshu, T. G. Forsthuber, G. Zhong, and B. P. Arulanandam**. 2008. Antigen-Specific $CD4^+$ T Cells Produce Sufficient IFN-gamma to Mediate Robust Protective Immunity against Genital *Chlamydia muridarum* Infection. J. Immunol. **180**:3375-3382.

19. **Darville, T., J. M. O'Neill, C. W. Andrews, Jr., U. M. Nagarajan, L. Stahl, and D. M. Ojcius**. 2003. Toll-like receptor-2, but not Toll-like receptor-4, is essential for development of oviduct pathology in chlamydial genital tract infection. J. Immunol. **171**:6187-6197.

20. **Imtiaz, M. T., J. H. Schripsema, I. M. Sigar, J. N. Kasimos, and K. H. Ramsey**. 2006. Inhibition of matrix metalloproteinases protects mice from ascending infection and

chronic disease manifestations resulting from urogenital *Chlamydia muridarum* infection. Infect. Immun. **74**:5513-5521.

21. **Wira, C. R., J. V. Fahey, C. L. Sentman, P. A. Pioli, and L. Shen**. 2005. Innate and adaptive immunity in female genital tract: cellular responses and interactions. Immunol. Rev. **206**:306-335.

22. **Maxion, H. K. and K. A. Kelly**. 2002. Chemokine expression patterns differ within anatomically distinct regions of the genital tract during *Chlamydia trachomatis* infection. Infect. Immun. **70**:1538-1546.

23. **Kelly, K. A., J. C. Walker, S. H. Jameel, H. L. Gray, and R. G. Rank**. 2000. Differential regulation of CD4 lymphocyte recruitment between the upper and lower regions of the genital tract during *Chlamydia trachomatis* infection. Infect. Immun. **68**:1519-1528.

24. **Berry, L. J., D. K. Hickey, K. A. Skelding, S. Bao, A. M. Rendina, P. M. Hansbro, C. M. Gockel, and K. W. Beagley**. 2004. Transcutaneous immunization with combined cholera toxin and CpG adjuvant protects against *Chlamydia muridarum* genital tract infection. Infect. Immun. **72**:1019-1028.

25. **Murphey, C., A. K. Murthy, P. A. Meier, G. M. Neal, G. Zhong, and B. P. Arulanandam**. 2006. The protective efficacy of chlamydial protease-like activity factor vaccination is dependent upon $CD4^+$ T cells. Cell Immunol. **242**:110-117.

26. **Morrison, S. G. and R. P. Morrison**. 2000. In situ analysis of the evolution of the primary immune response in murine *Chlamydia trachomatis* genital tract infection. Infect. Immun. **68**:2870-2879.

VITA

Ilea graduated from the United States Air Force Academy with a Bachelor of Science in Biology in May of 2007, receiving her commission as a 2nd Lieutenant in the United States Air Force. Ilea will serve the Air Force as a Scientist and hopes to return to the Air Force Academy to teach Biology.